Photochemical & Photobiological Sciences (2024) 23:421–434
https://doi.org/10.1007/s43630-023-00528-9

ORIGINAL PAPERS

Supramolecular chirality in self-assembly of zinc protobacteriochlorophyll-*d* analogs possessing enantiomeric esterifying groups

Mizuki Yasui[1] · **Hitoshi Tamiaki**[1]

Received: 31 October 2023 / Accepted: 19 December 2023 / Published online: 24 January 2024

Abstract

Zinc 3-hydroxymethyl-pyroprotopheophorbides-*a* esterified with a chiral secondary alcohol at the 17-propionate residue were prepared as bacteriochlorophyll-*d* analogs. The synthetic zinc 3^1-hydroxy-13^1-oxo-porphyrins self-aggregated in an aqueous Triton X-100 micellar solution to give red-shifted and broadened Soret and Qy absorption bands in comparison with their monomeric bands. The intense, exciton-coupled circular dichroism spectra of their self-aggregates were dependent on the chirality of the esterifying groups. The observation indicated that the self-aggregates based on the J-type stacking of the porphyrin cores were sensitive to the peripheral 17-propionate residues. The supramolecular structures of the present J-aggregates as models of bacteriochlorophyll aggregates in natural chlorosomes were remotely regulated by the esterifying groups.

Graphical abstract

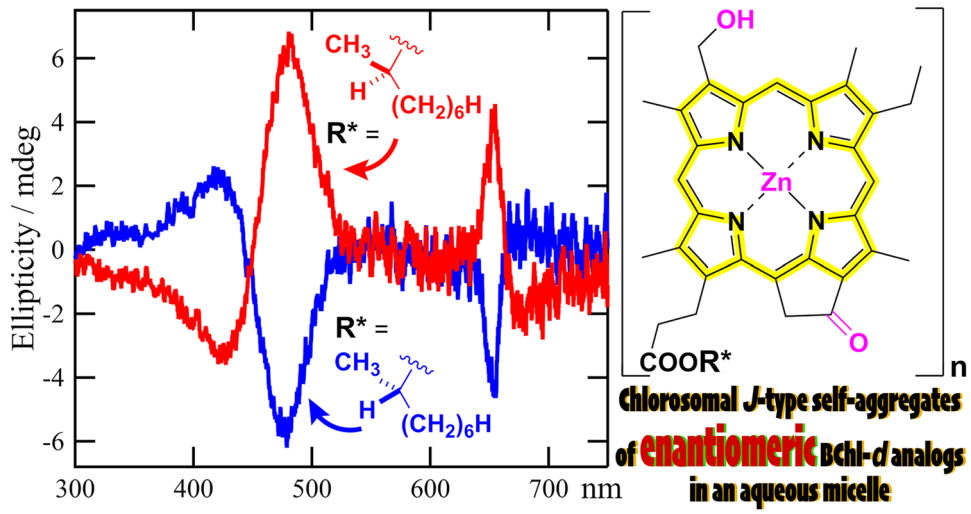

Keywords Chlorosome · Circular dichroism · Porphyrin · Self-aggregation · Substitution effect

1 Introduction

Light-harvesting antennas in phototrophs are generally composed of supramolecules of pigments with peptides. Most antenna systems in chlorophotosynthetic organisms are formed by the specific interaction of chlorophyll (Chl) or

✉ Hitoshi Tamiaki
tamiaki@fc.ritsumei.ac.jp

[1] Graduate School of Life Sciences, Ritsumeikan University, Kusatsu, Shiga 525-8577, Japan

bacteriochlorophyll (BChl) molecules with oligopeptides: typically see recent reports [1–19]. In contrast to the conventional photosynthetic antennas, green sulfur bacteria (GSB), filamentous anoxygenic phototrophs (FAP), and chloracidobacteria possess unique antenna systems, called chlorosomes, which are built up by the self-aggregation of BChl pigments without any interaction with peptides [20–23]. As chlorosomal pigments in GSB, farnesylated BChl-*c* or *d* molecules (R = farnesyl group in the left drawing of Fig. 1) are often observed [24]. Such BChls-*c*/*d* are a homologous mixture in the 8- and 12-substituents where further methylation occurs at the 8^2- and 12^1-positions and an epimeric mixture at the 3^1-position [25, 26]. Since the stereochemical configurations at the 17- and 18-positions are fixed to be (17*S*,18*S*)-stereochemistry, the 3^1-epimerization produces their diastereomeric mixtures [27, 28]. The 3^1-chiral position hardly affects the optical properties in their monomeric states due to its connection with the core chlorin π-system through the rotational C3–C3^1 bond [29, 30]. The 3^1-hydroxy group of one molecule is coordinated to the central magnesium atom of another molecule and hydrogen-bonded with the 13-carbonyl group of the third molecule to form the chlorosomal self-aggregates with π–π stacking of the composite chlorin chromophores [22, 23, 31]. Therefore, the 3^1-chirality influences the supramolecular structures of BChl-*c*/*d* self-aggregates and controls their optical properties including electronic absorption and emission data as well as circular dichroism (CD) [32, 33].

To reveal the effect of the 3^1-chirality on the self-aggregation, the 17,18-didehydrogenated analogs of BChl-*d*, zinc (1-hydroxyethyl)oxoporphyrins, were previously prepared as enantiomeric mixtures with a single chiral center in a molecule [34–36]. The enantiomerically pure models were produced via the separation by high performance liquid chromatography (HPLC) and self-aggregated in nonpolar organic solvents to give chlorosomal self-aggregates whose supramolecules were dependent on the chirality. As expected, the self-aggregates of the enantiomers exhibited intense CD spectra which were inverted by the epimerization. The phenomena are reasonable because the chiral carbon atom bearing the coordinating and hydrogen-bonding hydroxy group is directly connected with the porphyrin molecule which intermolecularly stacks via π–π interaction to form the aggregates. Since the esterifying group (R) in the 17-propionate residue is far from the chlorin chromophore in a molecule, we considered whether the R moiety could regulate the supramolecular structure or not.

Whereas GSB usually utilize BChls-*c*/*d* with a farnesyl group at the esterifying group (vide supra), BChl-*c* molecules in FAP possess a variety of the R groups including stearyl and phytyl groups [24, 37]. Recently, BChls-*c* with several different esterifying groups were detected in a chloracidobacterium, whose molecular structures have not been determined yet [38–40]. The effect of the esterifying substituents on the chlorosomal self-aggregation has not been fully disclosed, but their hydrophobic interactions among the neighboring BChl molecules or between the BChl and lipid molecules of the chlorosomal surface are proposed [22, 24]. Addition of some aliphatic alcohols to the medium for culturing a GSB species, *Chlorobaculum tepidum*, partially changed the esterifying groups in the produced BChl-*c* molecules [41–44], and alteration of the conditions for culturing a FAP species, *Chloroflexus aurantiacus*, varied the ratio of BChls-*c* with different esterifying groups [45]. The modified chlorosomes shifted their visible absorption maxima from the intact ones, indicating that the esterifying group would regulate the supramolecular structures of the self-aggregates. In vitro, BChls-*c* esterifying with different alcohols self-aggregated to give red-shifted and broadened electronic absorption bands, which were dependent on the esterifying groups [46–48]. Moreover, self-aggregates of synthetic BChl-*d* models **2** (Fig. 1, middle) exhibited chlorosomal absorption spectra in a variety of environments, which depended on the R groups [22, 24]. The hydrophobicity [49–54], hydrophilicity [50, 55], and fluorophilicity [56–58] of the

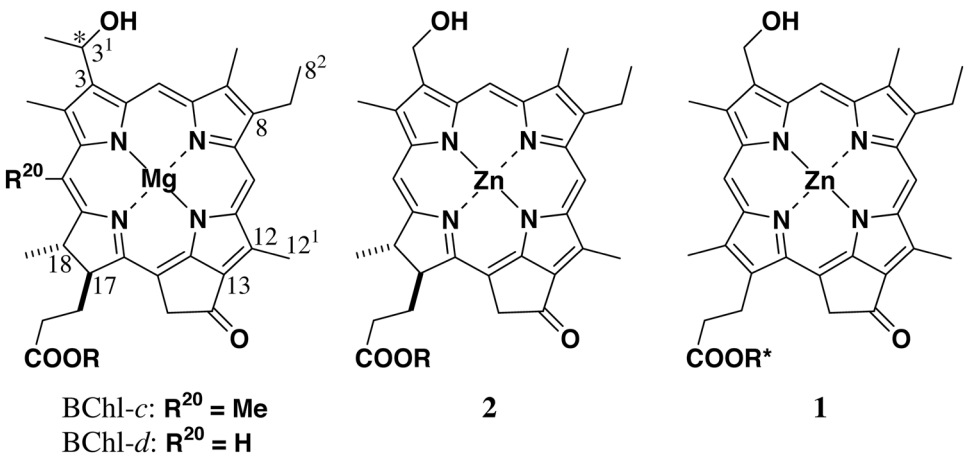

Fig. 1 Molecular structures of natural BChls-*c*/*d* (left) and their synthetic models with chlorin **2** (middle) and porphyrin π-skeletons **1** (right)

R moieties in **2** controlled the stability of the self-aggregates in less polar organic solvents, aqueous solution, and fluorous solvents (or liquid carbon dioxide), respectively.

To confirm the regulation of the chlorosomal self-aggregation by the esterifying group and its participation in the supramolecular structures, we herein report on the synthesis of BChl-*d* analogs **1** (Fig. 1, right) possessing a porphyrin π-skeleton and a chiral esterifying group (R*) and their self-aggregation in an aqueous micellar solution. The point chirality in the R* group was amplified in the self-aggregates to give intense, exciton-coupled, and chirality-dependent CD bands, indicating that the esterifying group regulated the supramolecular structure.

2 Experimental

2.1 General

Ultraviolet–visible (UV–Vis) absorption and CD spectra were measured with Hitachi U-4100 (Tokyo, Japan) and JASCO J-1500 spectrometers (Hachioji, Japan), respectively. ^{1}H NMR spectra were measured at room temperature with a JEOL ECA-600 (600 MHz) or AL400 (400 MHz) spectrometer (Akishima, Japan); chemical shifts (δs) are expressed in parts per million relative to residual chloroform (δ = 7.26 ppm) as an internal reference. Proton peaks were assigned using ^{1}H–^{1}H two-dimensional NMR techniques. High resolution mass spectra (HRMS) were recorded on a Bruker micrOTOF II spectrometer (Billerica, MA, USA): atmospheric pressure chemical ionization (APCI) and positive mode in acetonitrile. Flash column chromatography (FCC) was carried out with silica gel (Merck Kieselgel 60, 0.040–0.063 mm, Darmstadt, Germany). HPLC was performed on a packed octadecylated column (Inertsil ODS-P 5 µm, 10 mmϕ × 250 mm, GL Sciences, Tokyo, Japan) with Shimadzu LC-20AR pumps and SPD-M20A photodiode-array detector (Kyoto, Japan).

Pyropheophorbide-*a* (**6**) [59, 60] and its methyl ester (**7**) [61–64] were prepared according to reported procedures. All the reaction reagents and solvents were obtained from commercial suppliers and utilized as supplied. Especially, chiral methylcarbinols were purchased from TCI (Tokyo, Japan). Dry dichloromethane for esterification was obtained from FUJIFILM Wako Pure Chem. (Osaka, Japan) as reagent for organic synthesis as super dehydrated grade. Distilled water was prepared by a Yamato AutoStill WG250 system (Tokyo, Japan). Triton X-100 was purchased from Nacalai Tesque (Kyoto, Japan) and used as received. For optical spectroscopy, tetrahydrofuran (THF) was purchased from Nacalai Tesque as reagent prepared specially for HPLC.

2.2 Synthesis of pyropheophorbides-*a* 5aR/S–5cR/S

Carboxylic acid **6** (240.6 mg, 450 µmol) was dissolved into dry dichloromethane (30 ml) in the dark under argon at room temperature. The solution was cooled down in an ice bath, to which chiral methylcarbinol (2.25 mmol, 5 eq.), 1-[3-(*N*,*N*-dimethylamino)propyl]-3-ethylcarbodiimide hydrogen chloride (EDC·HCl, 431.3 mg, 2.25 mmol, 5 eq.), and 4-(*N*,*N*-dimethylamino)pyridine (DMAP, 549.8 mg, 4.5 mmol, 10 eq.) were added and stirred for 15 min. The mixed solution was further stirred for 15 h at room temperature. The reaction mixture was washed with an aqueous 1% hydrogen chloride solution, an aqueous solution saturated with sodium hydrogen carbonate, and brine, dried over sodium sulfate, and filtered. All the solvent was evaporated, and the residue was purified by FCC with dichloromethane and 0–3% diethyl ether to give the corresponding ester **5**.

(*R*)-2-Butyl pyropheophorbide-*a* (**5aR**): Esterification of **6** with (*R*)-2-butanol (206.9 µl) gave the titled ester (194.1 mg, 329 µmol, 73%): black solid; mp 199–200 °C; VIS (CH_2Cl_2) λ_{max}/nm = 668 (relative intensity, 0.43), 610 (0.08), 560 (0.03), 539 (0.09), 508 (0.11), 476 (0.04), 414 (1.00), 399 (0.81), 379 (0.54), 321 (0.22); ^{1}H NMR ($CDCl_3$, 600 MHz) δ/ppm = 9.45 (1H, s, 10-H), 9.33 (1H, s, 5-H), 8.55 (1H, s, 20-H), 7.98 (1H, dd, *J* = 18, 11.5 Hz, 3^1-H), 6.25 (1H, dd, *J* = 18, 1 Hz, 3^2-H *trans* to C3^1–H), 6.15 (1H, dd, *J* = 11.5, 1 Hz, 3^2-H *cis* to C3^1–H), 5.27, 5.11 (each 1H, d, *J* = 20 Hz, 13^1-CH_2), 4.81 (1H, sextet, *J* = 6 Hz, 17^2-COOCH), 4.50 (1H, dq, *J* = 2, 7 Hz, 18-H), 4.30 (1H, dt, *J* = 9, 2 Hz, 17-H), 3.65 (3H, s, 12-CH_3), 3.64 (2H, q, *J* = 8 Hz, 8-CH_2), 3.40 (3H, s, 2-CH_3), 3.20 (3H, s, 7-CH_3), 2.74–2.65, 2.58–2.49 (each 1H, m, 17^1-CH_2), 2.35–2.22 (2H, m, 17-CH_2), 1.81 (3H, d, *J* = 7 Hz, 18-CH_3), 1.68 (3H, t, *J* = 8 Hz, 8^1-CH_3), 1.52–1.39 (2H, m, 17^2-$COOCCH_2$), 1.15 (3H, d, *J* = 6 Hz, 17^2-$COOCCH_3$), 0.78 (3H, t, *J* = 7 Hz, 17^2-$COOC_2CH_3$), − 0.09, − 2.04 (each 1H, br-s, NH × 2); HRMS (APCI) found: *m*/*z* = 591.3326, calcd. for $C_{37}H_{43}N_4O_3$: MH^+, 591.3330.

(*S*)-2-Butyl pyropheophorbide-*a* (**5aS**): Esterification of **6** with (*S*)-2-butanol (206.9 µl) gave the titled ester (186.1 mg, 315 µmol, 70%): black solid; mp 200–201 °C; VIS (CH_2Cl_2) λ_{max}/nm = 668 (relative intensity, 0.43), 610 (0.08), 561 (0.03), 539 (0.09), 510 (0.10), 475 (0.04), 414 (1.00), 399 (0.81), 378 (0.53), 322 (0.20); ^{1}H NMR ($CDCl_3$, 400 MHz) δ/ppm = 9.44 (1H, s, 10-H), 9.33 (1H, s, 5-H), 8.55 (1H, s, 20-H), 7.98 (1H, dd, *J* = 18, 11 Hz, 3^1-H), 6.27 (1H, dd, *J* = 18, 1 Hz, 3^2-H *trans* to C3^1–H), 6.16 (1H, dd, *J* = 11, 1 Hz, 3^2-H *cis* to C3^1–H), 5.28, 5.12 (each 1H, d, *J* = 20 Hz, 13^1-CH_2), 4.86 (1H, sextet, *J* = 6 Hz, 17^2-COOCH), 4.51 (1H, dq, *J* = 2, 7 Hz, 18-H), 4.30 (1H, dt, *J* = 7, 2 Hz, 17-H), 3.65 (3H, s, 12-CH_3), 3.64 (2H, q, *J* = 8 Hz, 8-CH_2), 3.40 (3H, s, 2-CH_3), 3.20 (3H, s, 7-CH_3), 2.77–2.66, 2.61–2.49 (each 1H, m, 17^1-CH_2), 2.34–2.22 (2H, m, 17-CH_2), 1.83

(3H, d, $J = 7$ Hz, 18-CH_3), 1.67 (3H, t, $J = 8$ Hz, 8^1-CH_3), 1.53 (2H, m, 17^2-$COOCCH_2$), 1.15 (3H, d, $J = 6$ Hz, 17^2-$COOCCH_3$), 0.84 (3H, t, $J = 7$ Hz, 17^2-$COOC_2CH_3$), 0.42, − 1.72 (each 1H, br-s, NH × 2); HRMS (APCI) found: $m/z = 591.3320$, calcd. for $C_{37}H_{43}N_4O_3$: MH^+, 591.3330.

(*R*)-2-Octyl pyropheophorbide-*a* (**5bR**): Esterification of **6** with (*R*)-2-octanol (357.3 µl) gave the titled ester (203.8 mg, 315 µmol, 70%): black solid; mp 66–67 °C; VIS (CH_2Cl_2) λ_{max}/nm = 668 (relative intensity, 0.43), 609 (0.08), 561 (0.04), 539 (0.10), 510 (0.12), 477 (0.06), 414 (1.00), 399 (0.81), 379 (0.55), 321 (0.24); ^{1}H NMR ($CDCl_3$, 400 MHz) δ/ppm = 9.45 (1H, s, 10-H), 9.34 (1H, s, 5-H), 8.55 (1H, s, 20-H), 7.98 (1H, dd, $J = 18$, 12 Hz, 3^1-H), 6.26 (1H, dd, $J = 18$, 1 Hz, 3^2-H *trans* to C3^1–H), 6.16 (1H, dd, $J = 12$, 1 Hz, 3^2-H *cis* to C3^1–H), 5.28, 5.11 (each 1H, d, $J = 20$ Hz, 13^1-CH_2), 4.86 (1H, sextet, $J = 6$ Hz, 17^2-COOCH), 4.50 (1H, dq, $J = 2$, 7 Hz, 18-H), 4.30 (1H, dt, $J = 8$, 2 Hz, 17-H), 3.65 (3H, s, 12-CH_3), 3.65 (2H, q, $J = 8$ Hz, 8-CH_2), 3.40 (3H, s, 2-CH_3), 3.20 (3H, s, 7-CH_3), 2.75–2.64, 2.58–2.47 (each 1H, m, 17^1-CH_2), 2.35–2.20 (2H, m, 17-CH_2), 1.81 (3H, d, $J = 7$ Hz, 18-CH_3), 1.67 (3H, t, $J = 8$ Hz, 8^1-CH_3), 1.51–1.41, 1.41–1.31 (each 1H, m, 17^2-$COOCCH_2$), 1.26–1.18 (8H, m, 17^2-$COOC_2(CH_2)_4$), 1.15 (3H, d, $J = 6$ Hz, 17^2-$COOCCH_3$), 0.80 (3H, t, $J = 7$ Hz, 17^2-$COOC_6CH_3$), 0.42, − 1.73 (each 1H, br-s, NH × 2); HRMS (APCI) found: $m/z = 647.3977$, calcd. for $C_{41}H_{51}N_4O_3$: MH^+, 647.3956.

(*S*)-2-Octyl pyropheophorbide-*a* (**5bS**): Esterification of **6** with (*S*)-2-octanol (357.3 µl) gave the titled ester (212.5 mg, 328 µmol, 73%): black solid; mp 67–68 °C; VIS (CH_2Cl_2) λ_{max}/nm = 668 (relative intensity, 0.44), 610 (0.08), 560 (0.03), 539 (0.09), 509 (0.10), 476 (0.04), 414 (1.00), 400 (0.81), 380 (0.54), 323 (0.20); ^{1}H NMR ($CDCl_3$, 400 MHz) δ/ppm = 9.46 (1H, s, 10-H), 9.35 (1H, s, 5-H), 8.56 (1H, s, 20-H), 7.99 (1H, dd, $J = 18$, 12 Hz, 3^1-H), 6.27 (1H, dd, $J = 18$, 1 Hz, 3^2-H *trans* to C3^1–H), 6.16 (1H, dd, $J = 12$, 1 Hz, 3^2-H *cis* to C3^1–H), 5.28, 5.12 (each 1H, d, $J = 20$ Hz, 13^1-CH_2), 4.90 (1H, sextet, $J = 6$ Hz, 17^2-COOCH), 4.51 (1H, dq, $J = 2$, 7 Hz, 18-H), 4.30 (1H, dt, $J = 8$, 2 Hz, 17-H), 3.66 (3H, s, 12-CH_3), 3.66 (2H, q, $J = 8$ Hz, 8-CH_2), 3.41 (3H, s, 2-CH_3), 3.22 (3H, s, 7-CH_3), 2.75–2.65, 2.60–2.50 (each 1H, m, 17^1-CH_2), 2.33–2.22 (2H, m, 17-CH_2), 1.82 (3H, d, $J = 7$ Hz, 18-CH_3), 1.68 (3H, t, $J = 8$ Hz, 8^1-CH_3), 1.56–1.47, 1.46–1.35 (each 1H, m, 17^2-$COOCCH_2$), 1.28–1.08 (8H, m, 17^2-$COOC_2(CH_2)_4$), 1.14 (3H, d, $J = 7$ Hz, 17^2-$COOCCH_3$), 0.82 (3H, t, $J = 7$ Hz, 17^2-$COOC_6CH_3$), 0.44, − 1.71 (each 1H, br-s, NH × 2); HRMS (APCI) found: $m/z = 647.3955$, calcd. for $C_{41}H_{51}N_4O_3$: MH^+, 647.3956.

(*R*)-1-Phenylethyl pyropheophorbide-*a* (**5cR**): Esterification of **6** with (*R*)-1-phenylethanol (269.5 µl) gave the titled ester (224.2 mg, 351 µmol, 78%): black solid; mp 86–87 °C; VIS (CH_2Cl_2) λ_{max}/nm = 668 (relative intensity, 0.44), 610 (0.08), 559 (0.03), 539 (0.09), 509 (0.10), 477 (0.04), 414 (1.00), 400 (0.81), 380 (0.54), 323 (0.21); ^{1}H NMR ($CDCl_3$, 600 MHz) δ/ppm = 9.50 (1H, s, 10-H), 9.39 (1H, s, 5-H), 8.54 (1H, s, 20-H), 8.01 (1H, dd, $J = 18$, 11 Hz, 3^1-H), 7.29–7.22 (5H, m, 17^2-$COOCC_6H_5$), 6.29 (1H, dd, $J = 18$, 1 Hz, 3^2-H *trans* to C3^1–H), 6.17 (1H, dd, $J = 11$, 1 Hz, 3^2-H *cis* to C3^1–H), 5.88 (1H, q, $J = 6$ Hz, 17^2-COOCH), 5.22, 5.05 (each 1H, d, $J = 19$ Hz, 13^1-CH_2), 4.47 (1H, br-q, $J = 7$ Hz, 18-H), 4.27 (1H, br-d, $J = 9$ Hz, 17-H), 3.69 (2H, q, $J = 8$ Hz, 8-CH_2), 3.67 (3H, s, 12-CH_3), 3.41 (3H, s, 2-CH_3), 3.24 (3H, s, 7-CH_3), 2.72–2.67, 2.60–2.55 (each 1H, m, 17^1-CH_2), 2.31–2.25 (2H, m, 17-CH_2), 1.78 (3H, d, $J = 7$ Hz, 18-CH_3), 1.70 (3H, t, $J = 8$ Hz, 8^1-CH_3), 1.49 (3H, d, $J = 6$ Hz, 17^2-$COOCCH_3$), 0.45, − 1.69 (each 1H, br-s, NH × 2); HRMS (APCI) found: $m/z = 639.3325$, calcd. for $C_{41}H_{43}N_4O_3$: MH^+, 639.3330.

(*S*)-1-Phenylethyl pyropheophorbide-*a* (**5cS**): Esterification of **6** with (*S*)-1-phenylethanol (269.5 µl) gave the titled ester (253.0 mg, 396 µmol, 88%): black solid; mp 87–88 °C; VIS (CH_2Cl_2) λ_{max}/nm = 668 (relative intensity, 0.44), 610 (0.08), 559 (0.03), 540 (0.09), 510 (0.10), 477 (0.04), 415 (1.00), 400 (0.80), 379 (0.53), 322 (0.21); ^{1}H NMR ($CDCl_3$, 400 MHz) δ/ppm = 9.46 (1H, s, 10-H), 9.35 (1H, s, 5-H), 8.52 (1H, s, 20-H), 7.99 (1H, dd, $J = 18$, 12 Hz, 3^1-H), 7.28–7.21 (5H, m, 17^2-$COOCC_6H_5$), 6.27 (1H, dd, $J = 18$, 1 Hz, 3^2-H *trans* to C3^1–H), 6.16 (1H, dd, $J = 12$, 1 Hz, 3^2-H *cis* to C3^1–H), 5.86 (1H, q, $J = 7$ Hz, 17^2-COOCH), 5.24, 5.07 (each 1H, d, $J = 20$ Hz, 13^1-CH_2), 4.45 (1H, dq, $J = 2$, 7 Hz, 18-H), 4.26 (1H, dt, $J = 8$, 2 Hz, 17-H), 3.66 (2H, q, $J = 7$ Hz, 8-CH_2), 3.66 (3H, s, 12-CH_3), 3.39 (3H, s, 2-CH_3), 3.21 (3H, s, 7-CH_3), 2.71–2.63, 2.58–2.50 (each 1H, m, 17^1-CH_2), 2.35–2.21 (2H, m, 17-CH_2), 1.77 (3H, d, $J = 7$ Hz, 18-CH_3), 1.68 (3H, t, $J = 7$ Hz, 8^1-CH_3), 1.42 (3H, d, $J = 7$ Hz, 17^2-$COOCCH_3$), 0.43, − 1.75 (each 1H, br-s, NH × 2); HRMS (APCI) found: $m/z = 639.3345$, calcd. for $C_{41}H_{43}N_4O_3$: MH^+, 639.3330.

2.3 Synthesis of pyropheophorbides-*d* 4aR/S–4cR/S

Olefin **5** (350 µmol) was dissolved into THF (50 ml) in the dark under nitrogen at room temperature, to which one piece of osmium tetroxide, distilled water (1 ml), sodium periodate (374.3 mg, 1.75 mmol), and acetic acid (1 ml) were added. After stirred for 15 h, the reaction mixture was diluted with dichloromethane (50 ml), washed with an aqueous solution saturated with sodium hydrogen carbonate and distilled water, dried over sodium sulfate, and filtered. All the solvents were evaporated, and the residue was purified by FCC with dichloromethane and 0–3% diethyl ether to give the corresponding aldehyde **4**.

(*R*)-2-Butyl pyropheophorbide-*d* (**4aR**): Oxidation of **5aR** (206.8 mg) gave the titled aldehyde (116.2 mg, 196 µmol, 56%): black solid; mp 114–115 °C; VIS (CH_2Cl_2) λ_{max}/nm = 695 (relative intensity, 0.80), 634

(0.09), 555 (0.16), 522 (0.14), 428 (1.00), 388 (0.84), 328 (0.28), 306 (0.29); ^{1}H NMR ($CDCl_3$, 600 MHz) δ/ppm = 11.48 (1H, s, 3-CHO), 10.17 (1H, s, 5-H), 9.49 (1H, s, 10-H), 8.81 (1H, s, 20-H), 5.34, 5.19 (each 1H, d, J = 19 Hz, 13^1-CH_2), 4.82 (1H, sextet, J = 6 Hz, 17^2-COOCH), 4.59 (1H, dq, J = 2, 8 Hz, 18-H), 4.39 (1H, dt, J = 9, 2 Hz, 17-H), 3.74 (3H, s, 2-CH_3), 3.67 (3H, s, 12-CH_3), 3.66, 3.62 (each 1H, dq, J = 15, 8 Hz, 8-CH_2), 3.23 (3H, s, 7-CH_3), 2.76–2.70, 2.60–2.53 (each 1H, m, 17^1-CH_2), 2.33–2.26 (2H, m, 17-CH_2), 1.86 (3H, d, J = 8 Hz, 18-CH_3), 1.67 (3H, t, J = 8 Hz, 8^1-CH_3), 1.52–1.39 (2H, m, 17^2-$COOCCH_2$), 1.16 (3H, d, J = 6 Hz, 17^2-$COOCCH_3$), 0.77 (3H, t, J = 8 Hz, 17^2-$COOC_2CH_3$), − 0.27, − 2.19 (each 1H, br-s, NH × 2); HRMS (APCI) found: m/z = 593.3134, calcd. for $C_{36}H_{41}N_4O_4$: MH^+, 593.3122.

(*S*)-2-Butyl pyropheophorbide-*d* (**4aS**): Oxidation of **5aS** (206.8 mg) gave the titled aldehyde (190.9 mg, 322 μmol, 92%): black solid; mp 111–112 °C; VIS (CH_2Cl_2) λ_{max}/nm = 695 (relative intensity, 0.77), 636 (0.11), 555 (0.17), 523 (0.16), 427 (1.00), 387 (0.90), 329 (0.35), 307 (0.35); ^{1}H NMR ($CDCl_3$, 400 MHz) δ/ppm = 11.48 (1H, s, 3-CHO), 10.16 (1H, s, 5-H), 9.48 (1H, s, 10-H), 8.81 (1H, s, 20-H), 5.35, 5.19 (each 1H, d, J = 20 Hz, 13^1-CH_2), 4.86 (1H, sextet, J = 6 Hz, 17^2-COOCH), 4.59 (1H, dq, J = 2, 7 Hz, 18-H), 4.38 (1H, dt, J = 9, 2 Hz, 17-H), 3.75 (3H, s, 2-CH_3), 3.67 (3H, s, 12-CH_3), 3.63 (2H, q, J = 8 Hz, 8-CH_2), 3.23 (3H, s, 7-CH_3), 2.80–2.69, 2.64–2.54 (each 1H, m, 17^1-CH_2), 2.35–2.22 (2H, m, 17-CH_2), 1.86 (3H, d, J = 7 Hz, 18-CH_3), 1.67 (3H, t, J = 8 Hz, 8^1-CH_3), 1.63–1.43 (2H, m, 17^2-$COOCCH_2$), 1.15 (3H, d, J = 6 Hz, 17^2-$COOCCH_3$), 0.85 (3H, t, J = 7 Hz, 17^2-$COOC_2CH_3$), − 0.27, − 2.20 (each 1H, br-s, NH × 2); HRMS (APCI) found: m/z = 593.3132, calcd. for $C_{36}H_{41}N_4O_4$: MH^+, 593.3122.

(*R*)-2-Octyl pyropheophorbide-*d* (**4bR**): Oxidation of **5bR** (226.4 mg) gave the titled aldehyde (165.8 mg, 256 μmol, 73%): black solid; mp 83–84 °C; VIS (CH_2Cl_2) λ_{max}/nm = 695 (relative intensity, 0.77), 635 (0.10), 555 (0.17), 522 (0.16), 428 (1.00), 388 (0.88), 329 (0.37), 307 (0.35); ^{1}H NMR ($CDCl_3$, 400 MHz) δ/ppm = 11.50 (1H, s, 3-CHO), 10.21 (1H, s, 5-H), 9.52 (1H, s, 10-H), 8.82 (1H, s, 20-H), 5.35, 5.19 (each 1H, d, J = 20 Hz, 13^1-CH_2), 4.87 (1H, sextet, J = 6 Hz, 17^2-COOCH), 4.59 (1H, dq, J = 2, 7 Hz, 18-H), 4.38 (1H, dt, J = 9, 2 Hz, 17-H), 3.76 (3H, s, 2-CH_3), 3.68 (3H, s, 12-CH_3), 3.66 (2H, q, J = 8 Hz, 8-CH_2), 3.25 (3H, s, 7-CH_3), 2.78–2.68, 2.63–2.49 (each 1H, m, 17^1-CH_2), 2.36–2.22 (2H, m, 17-CH_2), 1.86 (3H, d, J = 7 Hz, 18-CH_3), 1.68 (3H, t, J = 8 Hz, 8^1-CH_3), 1.51–1.41, 1.40–1.30 (each 1H, m, 17^2-$COOCCH_2$), 1.24–1.12 (8H, m, 17^2-$COOC_2(CH_2)_4$), 1.16 (3H, d, J = 6 Hz, 17^2-$COOCCH_3$), 0.81 (3H, t, J = 7 Hz, 17^2-$COOC_6CH_3$), − 0.23, − 2.16 (each 1H, br-s, NH × 2); HRMS (APCI) found: m/z = 649.3730, calcd. for $C_{40}H_{49}N_4O_4$: MH^+, 649.3748.

(*S*)-2-Octyl pyropheophorbide-*d* (**4bS**): Oxidation of **5bS** (226.4 mg) gave the titled aldehyde (168.1 mg, 259 μmol, 74%): black solid; mp 89–90 °C; VIS (CH_2Cl_2) λ_{max}/nm = 695 (relative intensity, 0.81), 633 (0.09), 555 (0.16), 522 (0.15), 429 (1.00), 388 (0.84), 329 (0.30), 308 (0.31); ^{1}H NMR ($CDCl_3$, 400 MHz) δ/ppm = 11.48 (1H, s, 3-CHO), 10.17 (1H, s, 5-H), 9.49 (1H, s, 10-H), 8.82 (1H, s, 20-H), 5.35, 5.19 (each 1H, d, J = 20 Hz, 13^1-CH_2), 4.91 (1H, sextet, J = 6 Hz, 17^2-COOCH), 4.59 (1H, br-q, J = 7 Hz, 18-H), 4.38 (1H, br-d, J = 8 Hz, 17-H), 3.75 (3H, s, 2-CH_3), 3.67 (3H, s, 12-CH_3), 3.63 (2H, q, J = 8 Hz, 8-CH_2), 3.23 (3H, s, 7-CH_3), 2.80–2.68, 2.64–2.52 (each 1H, m, 17^1-CH_2), 2.35–2.22 (2H, m, 17-CH_2), 1.86 (3H, d, J = 7 Hz, 18-CH_3), 1.67 (3H, t, J = 8 Hz, 8^1-CH_3), 1.56–1.48, 1.47–1.36 (each 1H, m, 17^2-$COOCCH_2$), 1.29–1.16 (8H, m, 17^2-$COOC_2(CH_2)_4$), 1.14 (3H, d, J = 6 Hz, 17^2-$COOCCH_3$), 0.82 (3H, t, J = 7 Hz, 17^2-$COOC_6CH_3$), − 0.27, − 2.19 (each 1H, br-s, NH × 2); HRMS (APCI) found: m/z = 649.3728, calcd. for $C_{40}H_{49}N_4O_4$: MH^+, 649.3748.

(*R*)-1-Phenylethyl pyropheophorbide-*d* (**4cR**): Oxidation of **5cR** (223.6 mg) gave the titled aldehyde (172.7 mg, 270 μmol, 77%): black solid; mp 121–122 °C; VIS (CH_2Cl_2) λ_{max}/nm = 695 (relative intensity, 0.79), 635 (0.09), 555 (0.17), 522 (0.16), 488 (0.08), 430 (1.00), 388 (0.85), 329 (0.34), 306 (0.36); ^{1}H NMR ($CDCl_3$, 600 MHz) δ/ppm = 11.50 (1H, s, 3-CHO), 10.21 (1H, s, 5-H), 9.52 (1H, s, 10-H), 8.81 (1H, s, 20-H), 7.30–7.23 (5H, m, 17^2-$COOCC_6H_5$), 5.90 (1H, q, J = 7 Hz, 17^2-COOCH), 5.29, 5.13 (each 1H, d, J = 20 Hz, 13^1-CH_2), 4.57 (1H, dq, J = 2, 7 Hz, 18-H), 4.36 (1H, dt, J = 9, 2 Hz, 17-H), 3.76 (3H, s, 2-CH_3), 3.68 (3H, s, 12-CH_3), 3.66, 3.64 (each 1H, dq, J = 13, 8 Hz, 8-CH_2), 3.26 (3H, s, 7-CH_3), 2.76–2.70, 2.65–2.60 (each 1H, m, 17^1-CH_2), 2.34–2.25 (2H, m, 17-CH_2), 1.84 (3H, d, J = 7 Hz, 18-CH_3), 1.70 (3H, t, J = 8 Hz, 8^1-CH_3), 1.52 (3H, d, J = 7 Hz, 17^2-$COOCCH_3$), − 0.25, − 2.17 (each 1H, br-s, NH × 2); HRMS (APCI) found: m/z = 641.3101, calcd. for $C_{40}H_{41}N_4O_4$: MH^+, 641.3122.

(*S*)-1-Phenylethyl pyropheophorbide-*d* (**4cS**): Oxidation of **5cS** (223.6 mg) gave the titled aldehyde (168.2 mg, 262 μmol, 75%): black solid; mp 120–121 °C; VIS (CH_2Cl_2) λ_{max}/nm = 695 (relative intensity, 0.81), 635 (0.09), 555 (0.16), 522 (0.15), 488 (0.06), 430 (1.00), 388 (0.84), 329 (0.30), 307 (0.31); ^{1}H NMR ($CDCl_3$, 400 MHz) δ/ppm = 11.49 (1H, s, 3-CHO), 10.20 (1H, s, 5-H), 9.52 (1H, s, 10-H), 8.79 (1H, s, 20-H), 7.28–7.22 (5H, m, 17^2-$COOCC_6H_5$), 5.87 (1H, q, J = 6 Hz, 17^2-COOCH), 5.31, 5.13 (each 1H, d, J = 20 Hz, 13^1-CH_2), 4.53 (1H, dq, J = 2, 8 Hz, 18-H), 4.35 (1H, dt, J = 7, 2 Hz, 17-H), 3.74 (3H, s, 2-CH_3), 3.68 (3H, s, 12-CH_3), 3.66 (2H, q, J = 8 Hz, 8-CH_2), 3.25 (3H, s, 7-CH_3), 2.75–2.66, 2.63–2.53 (each 1H, m, 17^1-CH_2), 2.34–2.24 (2H, m, 17-CH_2), 1.81 (3H, d, J = 8 Hz, 18-CH_3), 1.68 (3H, t, J = 8 Hz, 8^1-CH_3), 1.43 (3H, d, J = 6 Hz, 17^2-$COOCCH_3$), − 0.24, − 2.18 (each 1H, br-s,

NH × 2); HRMS (APCI) found: $m/z = 641.3099$, calcd. for $C_{40}H_{41}N_4O_4$: MH^+, 641.3122.

2.4 Synthesis of 3-hydroxymethyl-pyropheophorbides-*a* 3aR/S–3cR/S

Aldehyde **4** (200 μmol) was dissolved into dichloromethane (20 ml) in the dark under nitrogen at room temperature, to which *tert*-butylamine borane complex (69.6 mg, 800 μmol) was added. After stirred for 15 min, the reaction mixture was diluted with dichloromethane (50 ml), washed with an aqueous solution saturated with ammonium chloride, dried over sodium sulfate, and filtered. All the solvent was evaporated, and the residue was purified by FCC with dichloromethane and 0–2% methanol to give the corresponding alcohol **3**.

(*R*)-2-Butyl 3-devinyl-3-hydroxymethyl-pyropheophorbide-*a* (**3aR**): Reduction of **4aR** (118.5 mg) gave the titled alcohol (73.7 mg, 124 μmol, 62%): black solid; mp 249–250 °C; VIS (CH_2Cl_2) λ_{max}/nm = 663 (relative intensity, 0.48), 605 (0.08), 557 (0.04), 535 (0.10), 505 (0.11), 471 (0.05), 410 (1.00), 397 (0.80), 376 (0.57), 317 (0.22); ^{1}H NMR ($CDCl_3$, 400 MHz) δ/ppm = 9.29 (1H, s, 5-H), 9.18 (1H, s, 10-H), 8.47 (1H, s, 20-H), 5.75 (2H, s, 3-CH_2), 5.05, 4.93 (each 1H, d, J = 20 Hz, 13^1-CH_2), 4.83 (1H, sextet, J = 6 Hz, 17^2-COOCH), 4.39 (1H, dq, J = 2, 7 Hz, 18-H), 4.12 (1H, dt, J = 9, 2 Hz, 17-H), 3.56 (2H, q, J = 8 Hz, 8-CH_2), 3.45 (3H, s, 12-CH_3), 3.34 (3H, s, 2-CH_3), 3.17 (3H, s, 7-CH_3), 2.57–2.44 (2H, m, 17^1-CH_2), 2.27–2.17, 2.13–2.02 (each 1H, m, 17-CH_2), 1.72 (3H, d, J = 7 Hz, 18-CH_3), 1.61 (3H, t, J = 8 Hz, 8^1-CH_3), 1.55–1.39 (2H, m, 17^2-$COOCCH_2$), 1.16 (3H, d, J = 6 Hz, 17^2-$COOCCH_3$), 0.80 (3H, t, J = 7 Hz, 17^2-$COOC_2CH_3$), − 0.09, − 2.04 (each 1H, br-s, NH × 2) [The 3^1-OH signal was invisible.]; HRMS (APCI) found: m/z = 595.3279 calcd. for $C_{36}H_{43}N_4O_4$: MH^+, 595.3279.

(*S*)-2-Butyl 3-devinyl-3-hydroxymethyl-pyropheophorbide-*a* (**3aS**): Reduction of **4aS** (118.5 mg) gave the titled alcohol (91.6 mg, 154 μmol, 77%): black solid; mp 217–218 °C; VIS (CH_2Cl_2) λ_{max}/nm = 662 (relative intensity, 0.48), 605 (0.08), 559 (0.03), 536 (0.09), 506 (0.10), 471 (0.04), 410 (1.00), 395 (0.79), 376 (0.57), 318 (0.21); ^{1}H NMR ($CDCl_3$, 400 MHz) δ/ppm = 9.37 (1H, s, 5-H), 9.34 (1H, s, 10-H), 8.52 (1H, s, 20-H), 5.83 (2H, s, 3-CH_2), 5.15, 5.02 (each 1H, d, J = 20 Hz, 13^1-CH_2), 4.86 (1H, sextet, J = 6 Hz, 17^2-COOCH), 4.45 (1H, dq, J = 2, 7 Hz, 18-H), 4.20 (1H, dt, J = 9, 2 Hz, 17-H), 3.63 (2H, q, J = 8 Hz, 8-CH_2), 3.56 (3H, s, 12-CH_3), 3.39 (3H, s, 2-CH_3), 3.22 (3H, s, 7-CH_3), 2.67–2.46 (2H, m, 17^1-CH_2), 2.31–2.11 (2H, m, 17-CH_2), 1.77 (3H, d, J = 7 Hz, 18-CH_3), 1.66 (3H, t, J = 8 Hz, 8^1-CH_3), 1.61–1.43 (2H, m, 17^2-$COOCCH_2$), 1.16 (3H, d, J = 6 Hz, 17^2-$COOCCH_3$), 0.85 (3H, t, J = 7 Hz, 17^2-$COOC_2CH_3$), 0.10, − 1.92 (each 1H, br-s, NH × 2) [The 3^1-OH signal was invisible.]; HRMS (APCI) found: m/z = 595.3271 calcd. for $C_{36}H_{43}N_4O_4$: MH^+, 595.3279.

(*R*)-2-Octyl 3-devinyl-3-hydroxymethyl-pyropheophorbide-*a* (**3bR**): Reduction of **4bR** (129.8 mg) gave the titled alcohol (87.2 mg, 134 μmol, 67%): black solid; mp 101–102 °C; VIS (CH_2Cl_2) λ_{max}/nm = 663 (relative intensity, 0.47), 605 (0.08), 557 (0.04), 536 (0.10), 505 (0.11), 470 (0.05), 410 (1.00), 397 (0.83), 377 (0.58), 319 (0.22); ^{1}H NMR ($CDCl_3$, 400 MHz) δ/ppm = 9.32 (1H, s, 5-H), 9.27 (1H, s, 10-H), 8.50 (1H, s, 20-H), 5.78 (2H, s, 3-CH_2), 5.11, 5.00 (each 1H, d, J = 20 Hz, 13^1-CH_2), 4.88 (1H, sextet, J = 7 Hz, 17^2-COOCH), 4.42 (1H, br-q, J = 7 Hz, 18-H), 4.17 (1H, br-d, J = 9 Hz, 17-H), 3.60 (2H, q, J = 7 Hz, 8-CH_2), 3.51 (3H, s, 12-CH_3), 3.36 (3H, s, 2-CH_3), 3.19 (3H, s, 7-CH_3), 2.61–2.45 (2H, m, 17^1-CH_2), 2.26–2.09 (2H, m, 17-CH_2), 1.75 (3H, d, J = 7 Hz, 18-CH_3), 1.64 (3H, t, J = 7 Hz, 8^1-CH_3), 1.53–1.44, 1.42–1.33 (each 1H, m, 17^2-$COOCCH_2$), 1.25–1.13 (8H, m, 17^2-$COOC_2(CH_2)_4$), 1.16 (3H, d, J = 7 Hz, 17^2-$COOCCH_3$), 0.81 (3H, t, J = 7 Hz, 17^2-$COOC_6CH_3$), − 1.98 (each 1H, br-s, NH) [Another inner NH and the 3^1-OH signals were invisible.]; HRMS (APCI) found: m/z = 651.3879, calcd. for $C_{40}H_{51}N_4O_4$: MH^+, 651.3905.

(*S*)-2-Octyl 3-devinyl-3-hydroxymethyl-pyropheophorbide-*a* (**3bS**): Reduction of **4bS** (129.8 mg) gave the titled alcohol (113.3 mg, 174 μmol, 87%): black solid; mp 101–102 °C; VIS (CH_2Cl_2) λ_{max}/nm = 662 (relative intensity, 0.48), 605 (0.08), 558 (0.03), 536 (0.09), 505 (0.10), 472 (0.04), 411 (1.00), 397 (0.78), 377 (0.56), 318 (0.21); ^{1}H NMR ($CDCl_3$, 400 MHz) δ/ppm = 9.38 (1H, s, 5-H), 9.37 (1H, s, 10-H), 8.53 (1H, s, 20-H), 5.85 (2H, s, 3-CH_2), 5.18, 5.03 (each 1H, d, J = 20 Hz, 13^1-CH_2), 4.91 (1H, sextet, J = 6 Hz, 17^2-COOCH), 4.46 (1H, dq, J = 2, 7 Hz, 18-H), 4.20 (1H, dt, J = 9, 2 Hz, 17-H), 3.64 (2H, q, J = 8 Hz, 8-CH_2), 3.57 (3H, s, 12-CH_3), 3.39 (3H, s, 2-CH_3), 3.22 (3H, s, 7-CH_3), 2.67–2.58, 2.54–2.48 (each 1H, m, 17^1-CH_2), 2.30–2.11 (2H, m, 17-CH_2), 1.78 (3H, d, J = 7 Hz, 18-CH_3), 1.66 (3H, t, J = 8 Hz, 8^1-CH_3), 1.56–1.47, 1.46–1.37 (each 1H, m, 17^2-$COOCCH_2$), 1.29–1.12 (8H, m, 17^2-$COOC_2(CH_2)_4$), 1.15 (3H, d, J = 7 Hz, 17^2-$COOCCH_3$), 0.82 (3H, t, J = 7 Hz, 17^2-$COOC_6CH_3$), 0.12, − 1.90 (each 1H, br-s, NH × 2) [The 3^1-OH signal was invisible.]; HRMS (APCI) found: m/z = 651.3880, calcd. for $C_{40}H_{51}N_4O_4$: MH^+, 651.3905.

(*R*)-1-Phenylethyl 3-devinyl-3-hydroxymethyl-pyropheophorbide-*a* (**3cR**): Reduction of **4cR** (128.2 mg) gave the titled alcohol (124.7 mg, 194 μmol, 97%): black solid; mp 137–138 °C; VIS (CH_2Cl_2) λ_{max}/nm = 663 (relative intensity, 0.48), 604 (0.08), 556 (0.03), 536 (0.09), 505 (0.10), 473 (0.04), 410 (1.00), 397 (0.80), 377 (0.56), 319 (0.21); ^{1}H NMR ($CDCl_3$, 600 MHz) δ/ppm = 9.44 (1H, s, 10-H), 9.41 (1H, s, 5-H), 8.53 (1H, s, 20-H), 7.29–7.21 (5H, m, 17^2-$COOCC_6H_5$), 5.89 (1H, q, J = 7 Hz, 17^2-COOCH),

5.88 (2H, s, 3-CH_2), 5.15, 5.00 (each 1H, d, J = 19 Hz, 13^1-CH_2), 4.45 (1H, dq, J = 2, 7 Hz, 18-H), 4.22 (1H, dt, J = 9, 2 Hz, 17-H), 3.67 (2H, q, J = 8 Hz, 8-CH_2), 3.62 (3H, s, 12-CH_3), 3.40 (3H, s, 2-CH_3), 3.25 (3H, s, 7-CH_3), 2.67–2.61, 2.59–2.54 (each 1H, m, 17^1-CH_2), 2.29–2.17 (2H, m, 17-CH_2), 2.18 (1H, br, 3^1-OH), 1.75 (3H, d, J = 7 Hz, 18-CH_3), 1.68 (3H, t, J = 8 Hz, 8^1-CH_3), 1.50 (3H, d, J = 7 Hz, 17^2-$COOCCH_3$), 0.18, − 1.86 (each 1H, br-s, NH × 2); HRMS (APCI) found: m/z = 643.3265, calcd. for $C_{40}H_{43}N_4O_4$: MH^+, 643.3279.

(*S*)-1-Phenylethyl 3-devinyl-3-hydroxymethyl-pyropheophorbide-*a* (**3cS**): Reduction of **4cS** (128.2 mg) gave the titled alcohol (124.7 mg, 194 μmol, 97%): black solid; mp 135–136 °C; VIS (CH_2Cl_2) λ_{max}/nm = 663 (relative intensity, 0.48), 606 (0.08), 557 (0.03), 536 (0.09), 506 (0.10), 475 (0.04), 410 (1.00), 397 (0.80), 377 (0.56), 317 (0.20); ^{1}H NMR ($CDCl_3$, 400 MHz) δ/ppm = 9.37 (1H, s, 5-H), 9.36 (1H, s, 10-H), 8.49 (1H, s, 20-H), 7.28–7.22 (5H, m, 17^2-$COOCC_6H_5$), 5.87 (1H, q, J = 7 Hz, 17^2-COOCH), 5.84 (2H, s, 3-CH_2), 5.13, 4.97 (each 1H, d, J = 20 Hz, 13^1-CH_2), 4.39 (1H, dq, J = 2, 7 Hz, 18-H), 4.17 (1H, dt, J = 8, 2 Hz, 17-H), 3.64 (2H, q, J = 7 Hz, 8-CH_2), 3.76 (3H, s, 12-CH_3), 3.57 (3H, s, 2-CH_3), 3.22 (3H, s, 7-CH_3), 2.62–2.48 (2H, m, 17^1-CH_2), 2.29–2.15 (2H, m, 17-CH_2), 1.72 (3H, d, J = 7 Hz, 18-CH_3), 1.67 (3H, t, J = 7 Hz, 8^1-CH_3), 1.44 (3H, d, J = 7 Hz, 17^2-$COOCCH_3$), 0.10, − 1.93 (each 1H, br-s, NH × 2) [The 3^1-OH signal was invisible.]; HRMS (APCI) found: m/z = 643.3263, calcd. for $C_{40}H_{43}N_4O_4$: MH^+, 643.3279.

2.5 Synthesis of zinc 3-hydroxymethyl-pyropheophorbides-*a* 2aR/S–2cR/S

Free base **3** (180 μmol) was dissolved into dichloromethane (20 ml) in the dark under nitrogen at room temperature, to which a methanol solution saturated with zinc acetate dihydrate (10 ml) was added. After stirred for 30 min, the reaction mixture was diluted with dichloromethane (30 ml), washed with an aqueous solution saturated with sodium hydrogen carbonate and distilled water, dried over sodium sulfate, and filtered. All the solvents were evaporated to give the corresponding zinc complex **2**.

Zinc (*R*)-2-butyl 3-devinyl-3-hydroxymethyl-pyropheophorbide-*a* (**2aR**): Zinc metalation of **3aR** (107.1 mg) gave the titled zinc complex (106.6 mg, 162 μmol, 90%): black solid; mp > 300 °C; VIS (THF) λ_{max}/nm = 646 (relative intensity, 0.74), 602 (0.10), 566 (0.06), 521 (0.03), 490 (0.02), 424 (1.00), 404 (0.57), 381 (0.31), 315 (0.20); ^{1}H NMR ($CDCl_3$–10% pyridine-d_5, 400 MHz) δ/ppm = 9.47 (1H, s, 10-H), 9.29 (1H, s, 5-H), 8.23 (1H, s, 20-H), 5.76 (2H, s, 3-CH_2), 5.10, 4.96 (each 1H, d, J = 20 Hz, 13^1-CH_2), 4.69 (1H, sextet, J = 6 Hz, 17^1-CH_2), 4.31 (1H, dq, J = 2.5, 7.5 Hz, 18-H), 4.10 (1H, dt, J = 8, 2.5 Hz, 17-H), 3.64 (2H, q, J = 7.5 Hz, 8-CH_2), 3.59 (3H, s, 12-CH_3), 3.19 (3H, s, 2-CH_3), 3.08 (3H, s, 7-CH_3), 2.52–2.41, 2.32–2.22 (each 1H, m, 17^1-CH_2), 2.21–2.09, 1.92–1.83 (each 1H, m, 17-CH_2), 1.62 (3H, d, J = 7.5 Hz, 18-CH_3), 1.59 (3H, t, J = 7.5 Hz, 8^1-CH_3), 1.36 (2H, m, 17^2-$COOCCH_2$), 1.02 (3H, d, J = 6 Hz, 17^2-$COOCCH_3$), 0.70 (3H, t, J = 7 Hz, 17^2-$COOC_2CH_3$) [The 3^1-OH signal was invisible.]; HRMS (APCI) found: m/z = 657.2392, calcd. for $C_{36}H_{41}N_4O_4Zn$: MH^+, 657.2414.

Zinc (*S*)-2-butyl 3-devinyl-3-hydroxymethyl-pyropheophorbide-*a* (**2aS**): Zinc metalation of **3aS** (107.1 mg) gave the titled zinc complex (109.0 mg, 166 μmol, 92%): black solid; mp 249–250 °C; VIS (THF) λ_{max}/nm = 646 (relative intensity, 0.74), 602 (0.11), 566 (0.06), 521 (0.04), 489 (0.02), 424 (1.00), 404 (0.58). 382 (0.32), 315 (0.23); ^{1}H NMR ($CDCl_3$–10% pyridine-d_5, 400 MHz) δ/ppm = 9.48 (1H, s, 10-H), 9.30 (1H, s, 5-H), 8.24 (1H, s, 20-H), 5.77 (2H, s, 3-CH_2), 5.11, 4.97 (each 1H, d, J = 20 Hz, 13^1-CH_2), 4.71 (1H, sextet, J = 6 Hz, 17^2-COOCH), 4.32 (1H, dq, J = 2, 7 Hz, 18-H), 4.11 (1H, dt, J = 8, 2 Hz, 17-H), 3.65 (2H, q, J = 8 Hz, 8-CH_2), 3.61 (3H, s, 12-CH_3), 3.21 (3H, s, 2-CH_3), 3.09 (3H, s, 7-CH_3), 2.53–2.42, 2.35–2.24 (each 1H, m, 17^1-CH_2), 2.21–2.10, 1.93–1.83 (each 1H, m, 17-CH_2), 1.63 (3H, d, J = 7 Hz, 18-CH_3), 1.60 (3H, t, J = 8 Hz, 8^1-CH_3), 1.39 (2H, m, 17^2-$COOCCH_2$), 1.04 (3H, d, J = 6 Hz, 17^2-$COOCCH_3$), 0.72 (3H, t, J = 7 Hz, 17^2-$COOC_2CH_3$) [The 3^1-OH signal was invisible.]; HRMS (APCI) found: m/z = 657.2389, calcd. for $C_{36}H_{41}N_4O_4Zn$: MH^+, 657.2414.

Zinc (*R*)-2-octyl 3-devinyl-3-hydroxymethyl-pyropheophorbide-*a* (**2bR**): Zinc metalation of **3bR** (117.2 mg) gave the titled zinc complex (91.3 mg, 128 μmol, 71%): black solid; mp 232–233 °C; VIS (THF) λ_{max}/nm = 646 (relative intensity, 0.73), 602 (0.11), 566 (0.06), 520 (0.04), 488 (0.03), 424 (1.00), 404 (0.57), 381 (0.33), 315 (0.26); ^{1}H NMR ($CDCl_3$–10% pyridine-d_5, 600 MHz) δ/ppm = 9.57 (1H, s, 10-H), 9.39 (1H, s, 5-H), 8.33 (1H, s, 20-H), 5.88, 5.84 (each 1H, d, J = 12 Hz, 3-CH_2), 5.20, 5.07 (each 1H, d, J = 19 Hz, 13^1-CH_2), 4.85 (1H, sextet, J = 6 Hz, 17^2-COOCH), 4.41 (1H, br-q, J = 7 Hz, 18-H), 4.20 (1H, br-d, J = 8 Hz, 17-H), 3.74 (2H, q, J = 8 Hz, 8-CH_2), 3.69 (3H, s, 12-CH_3), 3.29 (3H, s, 2-CH_3), 3.18 (3H, s, 7-CH_3), 2.59–2.53, 2.29–2.22 (each 1H, m, 17-CH_2), 2.39–2.33, 2.00–1.94 (each 1H, m, 17^1-CH_2), 1.72 (3H, d, J = 7 Hz, 18-CH_3), 1.69 (3H, t, J = 8 Hz, 8^1-CH_3), 1.51–1.45, 1.40–1.34 (each 1H, m, 17^2-$COOCCH_2$), 1.30–1.16 (8H, m, 17^2-$COOC_2(CH_2)_4$), 1.13 (3H, d, J = 6 Hz, 17^2-$COOCCH_3$), 0.83 (3H, t, J = 7 Hz, 17^2-$COOC_6CH_3$) [The 3^1-OH signal was invisible.]; HRMS (APCI) found: m/z = 713.3035, calcd. for $C_{40}H_{49}N_4O_4Zn$; MH^+, 713.3040.

Zinc (*S*)-2-octyl 3-devinyl-3-hydroxymethyl-pyropheophorbide-*a* (**2bS**): Zinc metalation of **3bS** (117.2 mg) gave the titled zinc complex (91.3 mg, 128 μmol, 71%): black

solid; mp 244–245 °C; VIS (THF) λ_{max}/nm = 646 (relative intensity, 0.74), 602 (0.11), 566 (0.06), 521 (0.04), 487 (0.03), 424 (1.00), 404 (0.57), 380 (0.32), 315 (0.23); ^{1}H NMR ($CDCl_3$–10% pyridine-d_5, 400 MHz) δ/ppm = 9.57 (1H, s, 10-H), 9.39 (1H, s, 5-H), 8.33 (1H, s, 20-H), 5.88, 5.84 (each 1H, d, J = 12 Hz, 3-CH_2), 5.21, 5.06 (each 1H, d, J = 20 Hz, 13^1-CH_2), 4.86 (1H, sextet, J = 6 Hz, 17^2-COOCH), 4.41 (1H, dq, J = 2, 7 Hz, 18-H), 4.20 (1H, dt, J = 8, 2 Hz, 17-H), 3.74 (2H, q, J = 8 Hz, 8-CH_2), 3.69 (3H, s, 12-CH_3), 3.29 (3H, s, 2-CH_3), 3.17 (3H, s, 7-CH_3), 2.62–2.51, 2.45–2.33 (each 1H, m, 17^1-CH_2), 2.30–2.19, 2.03–1.91 (each 1H, m, 17-CH_2), 1.72 (3H, d, J = 7 Hz, 18-CH_3), 1.69 (3H, t, J = 8 Hz, 8^1-CH_3), 1.55–1.45, 1.44–1.34 (each 1H, m, 17^2-$COOCCH_2$), 1.29–1.15 (8H, m, 17^2-$COOC_2(CH_2)_4$), 1.13 (3H, d, J = 6 Hz, 17^2-$COOCCH_3$), 0.83 (3H, t, J = 7 Hz, 17^2-$COOC_6CH_3$) [The 3^1-OH signal was invisible.]; HRMS (APCI) found: m/z = 713.3052, calcd. for $C_{40}H_{49}N_4O_4Zn$; MH^+, 713.3040.

Zinc (*R*)-1-phenylethyl 3-devinyl-3-hydroxymethyl-pyropheophorbide-*a* (**2cR**): Zinc metalation of **3cR** (115.7 mg) gave the titled zinc complex (123.4 mg, 175 μmol, 97%): black solid; mp > 300 °C; VIS (THF) λ_{max}/nm = 646 (relative intensity, 0.75), 602 (0.10), 566 (0.05), 521 (0.03), 488 (0.01), 424 (1.00), 404 (0.57), 380 (0.31), 315 (0.22); ^{1}H NMR ($CDCl_3$–10% pyridine-d_5, 600 MHz) δ/ppm = 9.56 (1H, s, 10-H), 9.38 (1H, s, 5-H), 8.31 (1H, s, 20-H), 7.30–7.21 (5H, m, 17^2-$COOCC_6H_5$), 5.85 (2H, s, 3-CH_2), 5.83 (1H, q, J = 7 Hz, 17^2-COOCH), 5.16, 5.02 (each 1H, d, J = 19 Hz, 13^1-CH_2), 4.37 (1H, dq, J = 2, 7 Hz, 18-H), 4.17 (1H, dt, J = 8, 3 Hz, 17-H), 3.74, 3.72 (each 1H, dq, J = 15, 8 Hz, 8-CH_2), 3.69 (3H, s, 12-CH_3), 3.29 (3H, s, 2-CH_3), 3.17 (3H, s, 7-CH_3), 2.58–2.52, 2.41–2.34 (each 1H, m, 17^1-CH_2), 2.30–2.22, 1.95–1.89 (each 1H, m, 17-CH_2), 1.69 (3H, d, J = 7 Hz, 18-CH_3), 1.69 (3H, t, J = 8 Hz, 8^1-CH_3), 1.46 (3H, d, J = 7 Hz, 17^2-$COOCCH_3$) [The 3^1-OH signal was invisible.]; HRMS (APCI) found: m/z = 705.2400, calcd. for $C_{40}H_{41}N_4O_4Zn$: MH^+, 705.2414.

Zinc (*S*)-1-phenylethyl 3-devinyl-3-hydroxymethyl-pyropheophorbide-*a* (**2cS**): Zinc metalation of **3cS** (115.7 mg) gave the titled zinc complex (123.3 mg, 175 μmol, 97%): black solid; mp 234–235 °C; VIS (THF) λ_{max}/nm = 646 (relative intensity, 0.73), 602 (0.11), 566 (0.06), 521 (0.04), 487 (0.03), 424 (1.00), 404 (0.58), 381 (0.33), 315 (0.26); ^{1}H NMR ($CDCl_3$–10% pyridine-d_5, 400 MHz) δ/ppm = 9.57 (1H, s, 10-H), 9.39 (1H, s, 5-H), 8.31 (1H, s, 20-H), 7.29–7.20 (5H, m, 17^2-$COOCC_6H_5$), 5.86 (2H, s, 3-CH_2), 5.82 (1H, q, J = 7 Hz, 17^2-COOCH), 5.18, 5.09 (each 1H, d, J = 20 Hz, 13^1-CH_2), 4.36 (1H, br-q, J = 7 Hz, 18-H), 4.17 (1H, dt, J = 8, 2 Hz, 17-H), 3.73 (2H, q, J = 7 Hz, 8-CH_2), 3.70 (3H, s, 12-CH_3), 3.29 (3H, s, 2-CH_3), 3.17 (3H, s, 7-CH_3), 2.57–2.50 (1H, m, 17^1-CH), 2.41–2.25 (2H, m, 17-CHCH), 1.96–1.88 (1H, m, 17-CH), 1.69 (3H, t, J = 7 Hz, 8^1-CH_3), 1.68 (3H, d, J = 7 Hz, 18-CH_3), 1.42 (3H, d, J = 7 Hz, 17^2-$COOCCH_3$) [The 3^1-OH signal was invisible.]; HRMS (APCI) found: m/z = 705.2394, calcd. for $C_{40}H_{41}N_4O_4Zn$; MH^+, 705.2413.

2.6 Synthesis of zinc 3-hydroxymethyl-pyroprotopheophorbides-*a* 1aR/S–1cR/S

Zinc chlorin **2** (100 μmol) was dissolved into pyridine (2 ml) in the dark under nitrogen at room temperature, to which an acetone solution (20 ml) of 2,3-dichloro-5,6-dicyano-1,4-benzoquinone (DDQ, 34.1 mg, 150 μmol) was added dropwise. After stirred for 10 min, the reaction mixture was diluted with chloroform (20 ml), washed with an aqueous 5% potassium hydrogen sulfate solution, an aqueous solution saturated with sodium hydrogen carbonate, brine, and distilled water, dried over sodium sulfate, and filtered. All the solvents were evaporated, and the residue was purified by HPLC with methanol and 5% pyridine to give the corresponding zinc porphyrin **1**. The isolated yields were at most 45%. Since the products were less soluble in deuterated solvents, their well-resolved proton peaks could not be obtained in ^{1}H NMR and the data are not shown below. Their purities were confirmed by HPLC (see Fig. S1).

Zinc (*R*)-2-butyl 3-devinyl-3-hydroxymethyl-pyroprotopheophorbide-*a* (**1aR**): Dehydrogenation of **2aR** gave the titled zinc porphyrin: black solid; mp 280–281 °C; VIS (THF) λ_{max}/nm = 609 (relative intensity, 0.11), 589 (0.04), 560 (0.06), 545 (0.04), 524 (0.03), 428 (1.00), 376 (0.13), 318 (0.13), 308 (0.12); HRMS (APCI) found: m/z = 655.2248, calcd. for $C_{36}H_{39}N_4O_4Zn$: MH^+, 655.2257.

Zinc (*S*)-2-butyl 3-devinyl-3-hydroxymethyl-pyroprotopheophorbide-*a* (**1aS**): Dehydrogenation of **2aS** gave the titled zinc complex: black solid; mp > 300 °C; VIS (THF) λ_{max}/nm = 609 (relative intensity, 0.10), 589 (0.03), 560 (0.05), 545 (0.03), 524 (0.02), 428 (1.00), 376 (0.12), 320 (0.09), 308 (0.12); HRMS (APCI) found: m/z = 655.2239, calcd. for $C_{36}H_{39}N_4O_4Zn$: MH^+, 655.2257.

Zinc (*R*)-2-octyl 3-devinyl-3-hydroxymethyl-pyroprotopheophorbide-*a* (**1bR**): Dehydrogenation of **2bR** gave the titled zinc porphyrin: black solid; mp 257–258 °C; VIS (THF) λ_{max}/nm = 609 (relative intensity, 0.11), 588 (0.03), 560 (0.05), 545 (0.03), 524 (0.02), 428 (1.00), 377 (0.12), 319(0.10), 309 (0.10); HRMS (APCI) found: m/z = 711.2866, calcd. for $C_{40}H_{47}N_4O_4Zn$: MH^+, 711.2883.

Zinc (*S*)-2-octyl 3-devinyl-3-hydroxymethyl-pyroprotopheophorbide-*a* (**1bS**): Dehydrogenation of **2bS** gave the titled zinc porphyrin: black solid; mp 254–255 °C; VIS (THF) λ_{max}/nm = 609 (relative intensity, 0.11), 588 (0.04), 560 (0.06), 545 (0.04), 524 (0.03), 428 (1.00), 376 (0.13), 319(0.12), 309 (0.12); HRMS (APCI) found: m/z = 711.2860, calcd. for $C_{40}H_{47}N_4O_4Zn$: MH^+, 711.2883.

Zinc (*R*)-1-phenylethyl 3-devinyl-3-hydroxymethyl-pyroprotopheophorbide-*a* (**1cR**): Dehydrogenation of **2cR** gave the titled zinc porphyrin: black solid; mp > 300 °C; VIS (THF) λ_{max}/nm = 609 (relative intensity, 0.11), 589 (0.03), 561 (0.05), 545 (0.03), 524 (0.02), 428 (1.00), 377 (0.12), 321(0.10), 307 (0.10); HRMS (APCI) found: *m*/*z* = 703.2254, calcd. for $C_{40}H_{39}N_4O_4Zn$: MH^+, 703.2257.

Zinc (*S*)-1-phenylethyl 3-devinyl-3-hydroxymethyl-pyroprotopheophorbide-*a* (**1cS**): Dehydrogenation of **2cS** gave the titled zinc porphyrin: black solid; mp > 300 °C; VIS (THF) λ_{max}/nm = 609 (relative intensity, 0.10), 589 (0.03), 560 (0.05), 545 (0.03), 524 (0.02), 428 (1.00), 377 (0.11), 321(0.09), 309 (0.08); HRMS (APCI) found: *m*/*z* = 703.2237, calcd. for $C_{40}H_{39}N_4O_4Zn$: MH^+, 703.2257.

3 Results and discussion

3.1 Synthesis of chiral zinc porphyrins

Zinc 3-hydroxymethyl-pyroprotopheophorbides-*a* **1aR/S–1cR/S** bearing a chiral esterifying group in the 17-propionate residue were prepared from naturally occurring Chl-*a* based on reported procedures [65]. Their synthetic route is briefly described below (Scheme 1). Methyl pyropheophorbide-*a* (**7**), one of the Chl-*a* derivatives, was acidically hydrolyzed [step (i), ≈100% isolated yield], and the resulting carboxylic acid **6** was esterified with commercially available, chiral methylcarbinols R*OH [$CH_3C^*H(OH)X$] under Steglich esterification conditions to give **5aR/S–5cR/S** [step (ii), 70% ~ 88%]. The 3-vinyl group of **5aR/S–5cR/S** was transformed into the formyl group in **4aR/S–4cR/S** under Lemieux–Johnson oxidation conditions [step (iii), 56% ~ 92%]. Aldehydes **4aR/S–4cR/S** were selectively reduced with a mild reducing reagent ($tBuNH_2BH_3$) to produce the corresponding alcohols **3aR/S–3cR/S** [step (iv), 62% ~ 97%]. Free bases **3aR/S–3cR/S** were zinc-metalated by a conventional procedure to afford zinc complexes **2aR/S–2cR/S** [step (v), 71% ~ 97%], which were successively 17,18-dehydrogenated by DDQ yielding zinc porphyrins **1aR/S–1cR/S** [step (vi), ≈45%]. The oxidized products were purified with HPLC to give enantiomerically pure samples of **1aR/S** [X = $(CH_2)_2H$], **1bR/S** [X = $(CH_2)_6H$], and **1cR/S** [X = C_6H_5] (Fig. 2) lacking their corresponding zinc chlorin precursors (Fig. S1). All the synthetic compounds were fully characterized by UV–Vis and/or ^1H NMR spectroscopy as well as mass spectrometry.

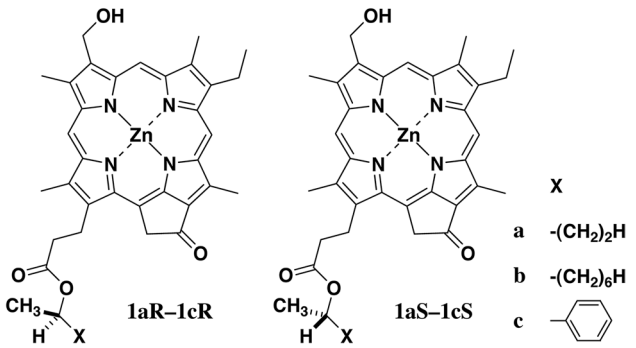

Fig. 2 Molecular structures of **1aR/S**, **1bR/S**, and **1cR/S**

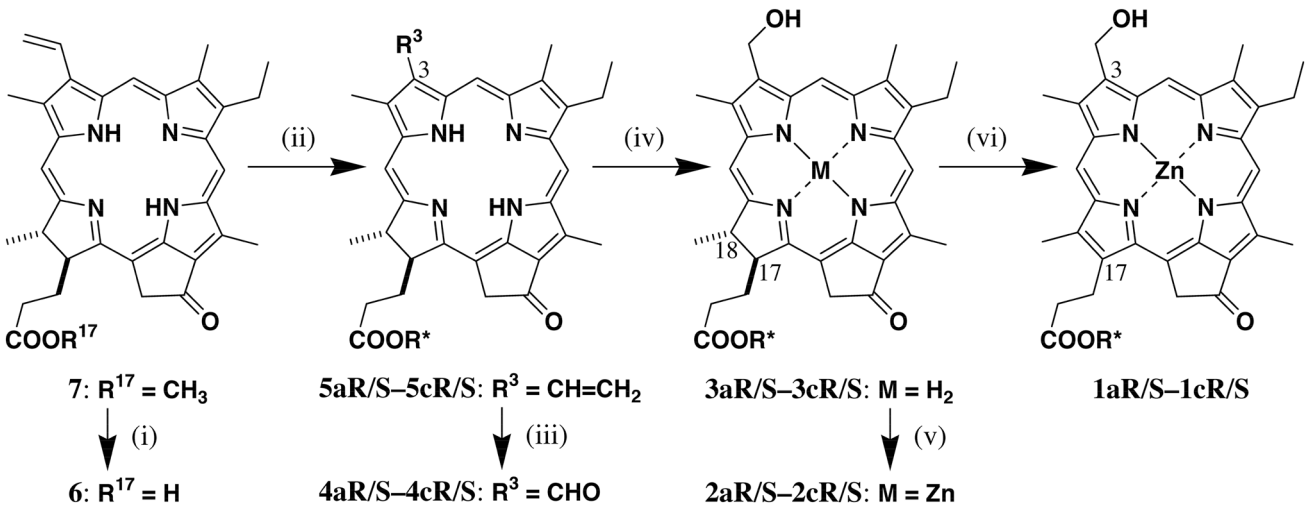

Scheme 1 Synthesis of zinc 3-hydroxymethyl-pyroprotopheophorbides-*a* **1aR/S–1cR/S** possessing a chiral esterifying group in the 17-propionate residue by chemically modifying a Chl-*a* derivative, methyl pyropheophorbide-*a* (**7**): (i) aq. HCl/Me_2CO; (ii) R*OH, EDC·HCl, DMAP/CH_2Cl_2; (iii) OsO_4, $NaIO_4$/aq. AcOH, THF; (iv) $tBuNH_2BH_3/CH_2Cl_2$; (v) $Zn(OAc)_2{\cdot}2H_2O$/MeOH, CH_2Cl_2; (vi) DDQ/Me_2CO, pyridine

3.2 Self-aggregation of chiral zinc porphyrins

Zinc porphyrin **1aR** bearing (*R*)-2-butyl ester was dissolved in THF to give a sharp UV–Vis absorption spectrum with the most intense peak at 428 nm as its Soret maximum and the second intense peak at 609 nm as its Qy maximum (see the black line in the upper panel of Fig. 3A). The spectral feature indicates that the central zinc of **1aR** was axially coordinated with a THF molecule and the resulting five-coordinated species was monomeric [34]. The solution exhibited no CD bands in the region of 300–750 nm (Fig. 3A, lower, black). The CD silence is ascribable to no electronic absorbance of its chiral ester moiety (COOC*H(CH_3)[(CH_2)$_2$H]) at the UV–Vis region.

The concentrated THF solution of **1aR** at 1 mM with 2.5%(wt/v) Triton X-100 was diluted with 99-fold distilled water to exhibit Soret and Qy absorption bands at ≈ 460 and 652 nm, respectively (Fig. 3A, upper, red). The absorption maxima moved to longer wavelengths than those of its monomeric species (vide supra). The red-shifted values of Soret and Qy maxima were ≈ 1600 and 1080 cm^{-1}, respectively. In addition, the red-shifted bands were broadened from the monomeric bands. The full widths at half maxima of the red-shifted Soret and Qy bands were ≈ 4000 and 680 cm^{-1}, respectively, to be larger than those of the monomeric bands (960 and 320 cm^{-1}). The red-shifted and broadened bands indicated that **1aR** self-aggregated via π–π stacking of the porphyrin cores in a J-type fashion similar to the chlorosomes [22]. Since **1aR** could not be dissolved in water, the molecule was situated inside the aqueous micelle prepared by Triton X-100 as one of the nonionic detergents. Therefore, chlorosomal self-aggregates of **1aR** were produced in the hydrophobic environment of aqueous Triton X-100 micelles. At the red-shifted Soret and Qy regions, apparent CD bands were observed (Fig. 3A, lower, red). An S-shaped CD band was visible at around 400 to 500 nm, and a less intense positive CD band was detected at the red-shifted Qy peak position. The observation is in sharp contrast to no CD band in the monomeric state. The self-aggregates of **1aR** were supramolecules with a chiral π–π stacking manner. The supramolecular chirality was produced by the (*R*)-2-butyl group in the 17-propionate residue far from the core porphyrin π–system in a molecule. The esterifying group affected the production of the supramolecular structures along with the 3^1-OH, central Zn, and 13-C=O moieties on the molecular y-axis mentioned in the Introduction section.

Enantiomeric isomer **1aS** possessing the (*S*)-2-butyl ester self-aggregated in an aqueous Triton X-100 solution to give red-shifted and broadened Soret and Qy bands being almost identical to those of the self-aggregated **1aR** (Fig. 3A, upper, blue and red lines). In the aqueous micellar solution, self-aggregates of **1aS** exhibited reverse S-shaped and relatively

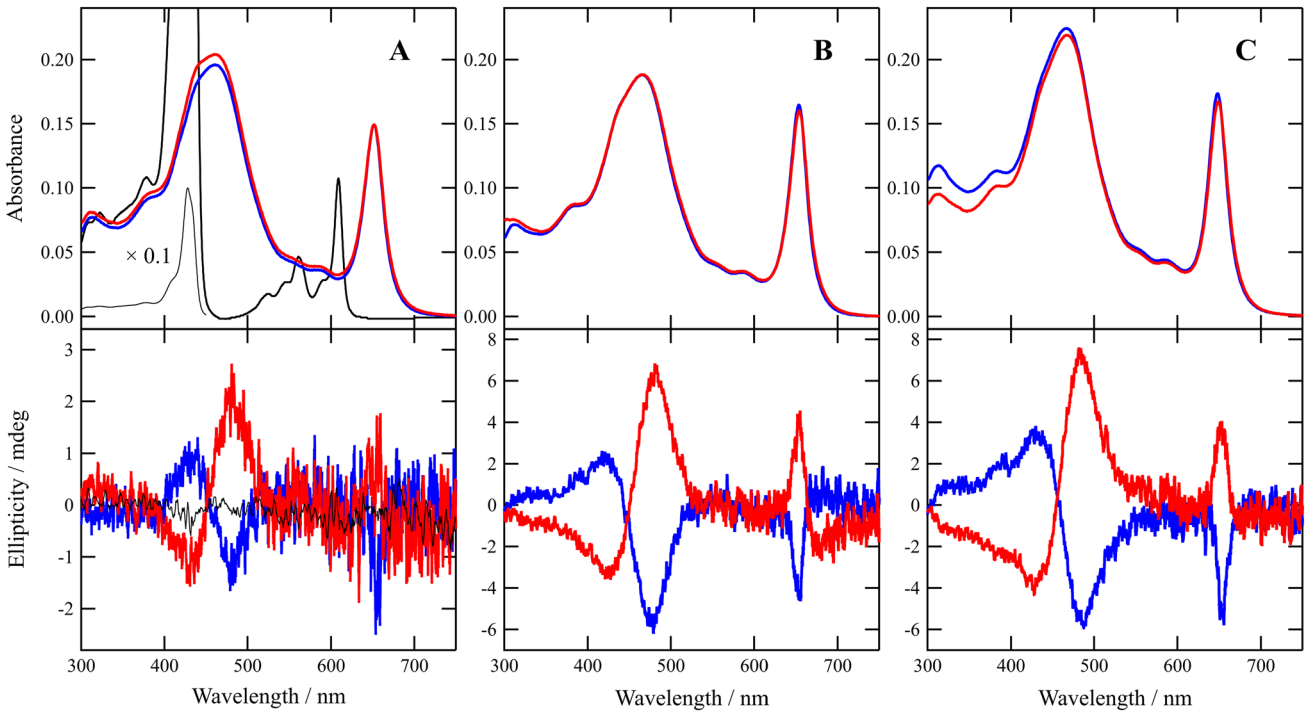

Fig. 3 UV–Vis absorption (upper) and CD spectra (lower) of **1aR/S** (A, red/blue lines), **1bR/S** (B, red/blue), and **1cR/S** (C, red/blue) in an aqueous 0.025%(wt/v) Triton X-100 solution containing 1%(v/v) THF as well as those of **1aR** in THF (A, black). The concentrations of the above samples were 10 μM

small negative CD bands at red-shifted Soret and Qy regions, respectively (Fig. 3A, lower, blue). The CD spectrum of **1aS** was opposite to that of **1aR**, confirming the supramolecular chirality by self-assembling enantiomerically pure **1aR/S** in the aqueous micelles.

As shown in the red line in the upper panel of Fig. 3B, self-aggregates of (*R*)-2-octyl ester **1bR** in the aqueous micellar solution showed a similar UV–Vis absorption spectrum to that of **1aR** self-aggregates. The red-shifted and broadened Soret and Qy bands indicated that **1bR** bearing a hexyl group (X in Fig. 2) at the asymmetric carbon atom self-aggregated similarly as **1aR** possessing an ethyl group at the same chiral center. The CD spectral feature of self-aggregated **1bR** also resembled that of $(\mathbf{1aR})_n$, but the former intensities were larger by approximately three times than the latter ones (Fig. 3B/A, lower, red lines). The triply elongation of the oligomethylene chain [$X = (CH_2)_2H \rightarrow (CH_2)_6H$] at the chiral center enhanced the CD intensities. The CD enhancement would be ascribable to an increase in the difference of the size between the alkyl groups (CH_3 and X in Fig. 2) on the chiral center, methyl (C_1) and ethyl groups (C_2) in **1aR** and methyl (C_1) and hexyl groups (C_6) in **1bR**. It is noted that a small but apparent dip was observed near 700 nm at the longer wavelength side of the positive CD band in **1bR**. As expected, **1bS** self-aggregated in the aqueous micellar solution to give the same red-shifted and broadened UV–Vis spectrum as in **1bR** and the CD spectrum of a reverse S-shaped band at the Soret region and a negative peak at the Qy region with a small damp at the redmost side which was reverse to that of **1bR**.

In the aqueous micellar solution, self-aggregates of (*R*)-1-phenylethyl ester **1cR** exhibited similar UV–Vis and CD spectra as in **1bR** (Fig. 3C/B, red). The effect of the former phenyl group at the asymmetric carbon atom on these spectra was nearly identical to that of the latter hexyl group with the same six carbon atoms. Stereochemical inversion of **1cR** to **1cS** hardly affected the UV–Vis spectra of their self-aggregates, but reversed the CD spectra (Fig. 3C, red to blue). The stereochemistry of the chiral secondary moieties [$C^*H(CH_3)X$] as the esterifying group in **1** regulated the supramolecular chirality of their self-aggregates in the aqueous micelles.

4 Conclusion

Zinc 3^1-demethyl-protobacteriochlorophylls-*d* possessing enantiomeric esterifying groups were prepared from naturally occurring Chl-*a*. The synthetic zinc complexes of fully π-conjugated porphyrins self-aggregated inside the hydrophobic environment of an aqueous Triton X-100 micelle, which were comparable to the chlorosomal self-aggregates of BChls-*c*/*d*. The supramolecular structures were constructed by the specific bonding of $Zn\cdots O3^2–H\cdots O=C13^1$ and π–π stacking of composite porphyrin cores [34], exhibiting red-shifted and broadened Soret and Qy bands similarly as in the natural chlorosomal J-aggregates.

The synthetic zinc 3-hydroxymethyl-porphyrins were enantiomers due to the single chirality in the 17-propionate residue. The self-aggregates of all the (*R*)-enantiomers in the aqueous micelles gave S-shaped bisignate and positive CD bands at the red-shifted and broadened Soret and Qy regions, respectively, while those of the (*S*)-stereoisomers afforded the reverse CD signs. The relatively intense CD bands based on the exciton-coupling of the porphyrin cores were dependent on the chirality of the substituents remote from the core. The supramolecular structures of the chlorosomal J-aggregates were controlled by the peripheral 17-propionate residue. The observation is comparable to the previous reports that the chiral peripheries of synthetic porphyrins regulated their assemblies [66].

Supplementary Information The online version contains supplementary material available at https://doi.org/10.1007/s43630-023-00528-9.

Acknowledgements We thank Messrs. Akihiro Tsuru, Hajime Sumi, and Jun Komada of Ritsumeikan University for their experimental assistance and Dr. Shin Ogasawara of Ritsumeikan University for preparation of drawings. This work was partially supported by JSPS KAKENHI Grant Numbers 22H02203 in Scientific Research (B) and 17H06436 in Scientific Research on Innovative Areas "Innovation for Light-Energy Conversion (I^4LEC)".

Funding Open Access funding provided by Ritsumeikan University. Japan Society for the Promotion of Science, 22H02203, Hitoshi Tamiaki, 17H06436, Hitoshi Tamiaki.

Data availability All data in this work are available on request from the corresponding author.

Declarations

Conflict of interest There are no conflicts of interest to declare.

References

1. Kimura, Y., Tani, K., Madigan, M. T., & Wang-Otomo, Z.-Y. (2023). Advances in the spectroscopic and structural characterization of core light-harvesting complexes from purple phototrophic

bacteria. *The Journal of Physical Chemistry B, 127*(1), 6–17. https://doi.org/10.1021/acs.jpcb.2c06638
2. Timpmann, K., Kangur, L., & Freiberg, A. (2023). Hysteretic pressure dependence of Ca^{2+} binding in LH1 bacterial membrane chromoproteins. *The Journal of Physical Chemistry B, 127*(2), 456–464. https://doi.org/10.1021/acs.jpcb.2c05938
3. Xie, H., Lyratzakis, A., Khera, R., Koutantou, M., Welsch, S., Michel, H., & Tsiotis, G. (2023). Cryo-EM structure of the whole photosynthetic reaction center apparatus from the green sulfur bacterium *Chlorobaculum tepidum*. *Proceedings of the National Academy of Sciences of the United States of America, 120*(5), e2216734120. https://doi.org/10.1073/pnas.2216734120
4. Chen, J.-H., Wang, W., Wang, C., Kuang, T., Shen, J.-R., & Zhang, X. (2023). Cryo-electron microscopy structure of the intact photosynthetic light-harvesting antenna-reaction center complex from a green sulfur bacterium. *Journal of Integrative Plant Biology, 65*(1), 223–234. https://doi.org/10.1111/jipb.13367
5. Kosugi, M., Kawasaki, M., Shibata, Y., Hara, K., Takaichi, S., Moriya, T., Adachi, N., Kamei, Y., Kashino, Y., Kudoh, S., Koike, H., & Senda, T. (2023). Uphill energy transfer mechanism for photosynthesis in an Antarctic alga. *Nature Communications, 14*, 730. https://doi.org/10.1038/s41467-023-36245-1
6. Saga, Y., Hamanishi, K., Yamamoto, T., Hinago, K., & Nagasawa, Y. (2023). Conversion of B800 bacteriochlorophyll *a* to 3-acetyl chlorophyll *a* in the light-harvesting complex 3 by in situ oxidation. *The Journal of Physical Chemistry B, 127*(12), 2683–2689. https://doi.org/10.1021/acs.jpcb.2c08887
7. Maity, S., & Kleinekathöfer, U. (2023). Recent progress in atomistic modeling of light-harvesting complexes: A mini review. *Photosynthesis Research, 156*(1), 147–162. https://doi.org/10.1007/s11120-022-00969-w
8. You, X., Zhang, X., Cheng, J., Xiao, Y., Ma, J., Sun, S., Zhang, X., Wang, H.-W., & Sui, S.-F. (2023). In situ structure of the red algal phycobilisome–PSII–PSI–LHC megacomplex. *Nature, 616*(7955), 199–206. https://doi.org/10.1038/s41586-023-05831-0
9. Bracun, L., Yamagata, A., Christianson, B. M., Shirouzu, M., & Liu, L.-N. (2023). Cryo-EM structure of a monomeric RC-LH1-PufX supercomplex with high-carotenoid content from *Rhodobacter capsulatus*. *Structure, 31*(3), 318–328. https://doi.org/10.1016/j.str.2023.01.006
10. Hitchcock, A., Swainsbury, D. J. K., & Hunter, C. N. (2023). Photosynthesis in the near infrared: The γ subunit of *Blastochloris viridis* LH1 red-shifts absorption beyond 1000 nm. *Biochemical Journal, 480*(6), 455–460. https://doi.org/10.1042/BCJ20220585
11. Dong, S., Huang, G., Wang, C., Wang, J., Sui, S.-F., & Qin, X. (2022). Structure of the Acidobacteria homodimeric reaction center bound with cytochrome *c*. *Nature Communications, 13*, 7745. https://doi.org/10.1038/s41467-022-35460-6
12. Morimoto, M., Hirao, H., Kondo, M., Dewa, T., Kimura, Y., Wang-Otomo, Z.-Y., Asakawa, H., & Saga, Y. (2023). Atomic force microscopic analysis of the light-harvesting complex 2 from purple photosynthetic bacterium *Thermochromatium tepidum*. *Photosynthesis Research, 157*(1), 13–20. https://doi.org/10.1007/s11120-023-01010-4
13. Otomo, K., Dewa, T., Matsushita, M., & Fujiyoshi, S. (2023). Cryogenic single-molecule fluorescence detection of the mid-infrared response of an intrinsic pigment in a light-harvesting complex. *The Journal of Physical Chemistry B, 127*(22), 4959–4965. https://doi.org/10.1021/acs.jpcb.3c00284
14. Rätsep, M., Lehtmets, A., Kangur, L., Timpmann, K., Leiger, K., Wang-Otomo, Z.-Y., & Freiberg, A. (2023). Evaluation of the relationship between color-tuning of photosynthetic excitons and thermodynamic stability of light-harvesting chromoproteins. *Photosynthetica, 61*(3), 308–317. https://doi.org/10.32615/ps.2023.022
15. Klinger, A., Lindorfer, D., Müh, F., & Renger, T. (2023). Living on the edge: Light-harvesting efficiency and photoprotection in the core of green sulfur bacteria. *Physical Chemistry Chemical Physics, 25*(28), 18698–18710. https://doi.org/10.1039/d3cp01321a
16. Elias, E., Liguori, N., & Croce, R. (2023). At the origin of the selectivity of the chlorophyll-binding sites in light harvesting complex II (LHCII). *International Journal of Biological Macromolecules, 243*, 125069. https://doi.org/10.1016/j.ijbiomac.2023.125069
17. González-Soria, B., & Delgado, F. (2023). Temperature dependence of entanglement and coherence in Fenna–Matthews–Olson complex. *Journal of Physics: Conference Series, 2448*, 012016. https://doi.org/10.1088/1742-6596/2448/1/012016
18. Swainsbury, D. J. K., Qian, P., Hitchcock, A., & Hunter, C. N. (2023). The structure and assembly of reaction centre-light-harvesting 1 complexes in photosynthetic bacteria. *Bioscience Reports, 43*(5), BSR20220089. https://doi.org/10.1042/BSR20220089
19. Thwaites, O., Christianson, B. M., Cowan, A. J., Jäckel, F., Liu, L.-N., & Gardner, A. M. (2023). Unravelling the roles of integral polypeptides in excitation energy transfer of photosynthetic RC-LH1 supercomplexes. *The Journal of Physical Chemistry B, 127*(33), 7283–7290. https://doi.org/10.1021/acs.jpcb.3c04466
20. Orf, G. S., & Blankenship, R. E. (2013). Chlorosome antenna complexes from green photosynthetic bacteria. *Photosynthesis Research, 116*(2–3), 315–331. https://doi.org/10.1007/s11120-013-9869-3
21. Otsuki, J. (2018). Supramolecular approach towards light-harvesting materials based on porphyrins and chlorophylls. *Journal of Materials Chemistry A, 6*(16), 6710–6753. https://doi.org/10.1039/c7ta11274b
22. Matsubara, S., & Tamiaki, H. (2020). Supramolecular chlorophyll aggregates inspired from specific light-harvesting antenna "chlorosome": Static nanostructure, dynamic construction process, and versatile application. *Journal of Photochemistry and Photobiology C: Photochemistry Reviews, 45*, 100385. https://doi.org/10.1016/j.jphotochemrev.2020.100385
23. Eric, V., Li, X., Dsouza, L., Frehan, S. K., Huijser, A., Holzwarth, A. R., Buda, F., Sevink, G. J. A., de Groot, H. J. M., & Jansen, T. L. C. (2023). Manifestation of hydrogen bonding and exciton delocalization on the absorption and two-dimensional electronic spectra of chlorosomes. *The Journal of Physical Chemistry B, 127*(5), 1097–1109. https://doi.org/10.1021/acs.jpcb.2c07143
24. Tamiaki, H., Shibata, R., & Mizoguchi, T. (2007). The 17-propionate function of (bacterio)chlorophylls: Biological implication of their long esterifying chains in photosynthetic systems. *Photochemistry and Photobiology, 83*(1), 152–162. https://doi.org/10.1562/2006-02-27-IR-819
25. Tsukatani, Y., Harada, J., Mizoguchi, T., & Tamiaki, H. (2013). Bacteriochlorophyll homolog compositions in the *bchU* mutants of green sulfur bacteria. *Photochemical & Photobiological Sciences, 12*(12), 2195–2201. https://doi.org/10.1039/c3pp50253h
26. Bryant, D. A., Hunter, C. N., & Warren, M. J. (2020). Biosynthesis of the modified tetrapyrroles—the pigments of life. *Journal of Biological Chemistry, 295*(20), 6888–6925. https://doi.org/10.1074/jbc.REV120.006194
27. Senge, M. O., Ryan, A. A., Letchford, K. A., MacGowan, S. A., & Mielke, T. (2014). Chlorophylls, symmetry, chirality, and photosynthesis. *Symmetry, 6*(3), 781–843. https://doi.org/10.3390/sym6030781
28. Tamiaki, H. (2022). Chlorophylls. In: P. J. Brothers & M. O. Senge (Eds.), *Fundamentals of porphyrin chemistry: A 21st century approach, chap 17* (Vol. 2, pp. 743–776). West Sussex: Wiley. https://doi.org/10.1002/9781119129301.ch17
29. Chiefari, J., Griebenow, K., Griebenow, N., Balaban, T. S., Holzwarth, A. R., & Schaffner, K. (1995). Models for the pigment

organization in the chlorosomes of photosynthetic bacteria: Diastereoselective control of *in-vitro* bacteriochlorophyll c_s aggregation. *The Journal of Physical Chemistry, 99*(4), 1357–1365. https://doi.org/10.1021/j100004a041
30. Balaban, T. S., Holzwarth, A. R., & Schaffner, K. (1995). Circular dichroism study on the diastereoselective self-assembly of bacteriochlorophyll c_s. *Journal of Molecular Structure, 349*, 183–186. https://doi.org/10.1016/0022-2860(95)08739-I
31. Ganapathy, S., Oostergetel, G. T., Wawrzyniak, P. K., Reus, M., Chew, A. G. M., Buda, F., Boekema, E. J., Bryant, D. A., Holzwarth, A. R., & de Groot, H. J. M. (2009). Alternating *syn-anti* bacteriochlorophylls form concentric helical nanotubes in chlorosomes. *Proceedings of the National Academy of Sciences of the United States of America, 106*(21), 8525–8530. https://doi.org/10.1073/pnas.0903534106
32. Harada, J., Teramura, M., Mizoguchi, T., Tsukatani, Y., Yamamoto, K., & Tamiaki, H. (2015). Stereochemical conversion of C3-vinyl group to 1-hydroxyethyl group in bacteriochlorophyll *c* by the hydratases BchF and BchV: Adaptation of green sulfur bacteria to limited-light environments. *Molecular Microbiology, 98*(6), 1184–1198. https://doi.org/10.1111/mmi.13208
33. Shoji, S., Mizoguchi, T., & Tamiaki, H. (2016). *In vitro* self-assemblies of bacteriochlorophylls-*c* from *Chlorobaculum tepidum* and their supramolecular nanostructures. *Journal of Photochemistry and Photobiology A: Chemistry, 331*, 190–196. https://doi.org/10.1016/j.jphotochem.2015.11.003
34. Tamiaki, H., Kitamoto, H., Watanabe, T., & Shibata, R. (2005). Self-aggregation of synthetic protobacteriochlorophyll-*d* derivatives. *Photochemistry and Photobiology, 81*(1), 170–176. https://doi.org/10.1111/j.1751-1097.2005.tb01537.x
35. Balaban, T. S., Linke-Schaetzel, M., Bhise, A. D., Vanthuyne, N., & Roussel, C. (2004). Green self-assembling porphyrins and chlorins as mimics of the natural bacteriochlorophylls *c*, *d*, and *e*. *European Journal of Organic Chemistry, 18*, 3919–3930. https://doi.org/10.1002/ejoc.200400151
36. Balaban, T. S., Bhise, A. D., Bringmann, G., Bürck, J., Chappaz-Gillot, C., Eichhöfer, A., Fenske, D., Götz, D. C. G., Knauer, M., Mizoguchi, T., Mössinger, D., Rösner, H., Roussel, C., Schraut, M., Tamiaki, H., & Vanthuyne, N. (2009). Mimics of the self-assembling chlorosomal bacteriochlorophylls: Regio- and stereoselective synthesis and stereoanalysis of acyl(1-hydroxyalkyl) porphyrins. *Journal of the American Chemical Society, 131*(40), 14480–14492. https://doi.org/10.1021/ja905628h
37. Fages, F., Griebenow, N., Griebenow, K., Holzwarth, A. R., & Schaffner, K. (1990). Characterization of light-harvesting pigments of *Chloroflexus aurantiacus.* Two new chlorophylls: Oleyl (octadec-9-enyl) and cetyl (hexadecanyl) bacteriochlorophyllide-c. *Journal of the Chemical Society, Perkin Transactions, 1*(10), 2791–2797. https://doi.org/10.1039/P19900002791
38. Bryant, D. A., Costas, A. M. G., Maresca, J. A., Chew, A. G. M., Klatt, C. G., Bateson, M. M., Tallon, L. J., Hostetler, J., Nelson, W. C., Heidelberg, J. F., & Ward, D. M. (2007). *Candidatus* Chloracidobacterium thermophilum: An aerobic phototrophic acidobacterium. *Science, 317*(5837), 523–526. https://doi.org/10.1126/science.1143236
39. Costas, A. M. G., Tsukatani, Y., Rijpstra, W. I. C., Schouten, S., Welander, P. V., Summons, R. E., & Bryant, D. A. (2012). Identification of the bacteriochlorophylls, carotenoids, quinones, lipids, and hopanoids of "*Candidatus* Chloracidobacterium thermophilum". *Journal of Bacteriology, 194*(5), 1158–1168. https://doi.org/10.1128/JB.06421-11
40. Tank, M., & Bryant, D. A. (2015). Nutrient requirements and growth physiology of the photoheterotrophic Acidobacterium. *Chloracidobacterium thermophilum. Frontiers in Microbiology, 6*, 226. https://doi.org/10.3389/fmicb.2015.00226
41. Steensgaard, D. B., Cox, R. P., & Miller, M. (1996). Manipulation of the bacteriochlorophyll *c* homolog distribution in the green sulfur bacterium *Chlorobium tepidum*. *Photosynthesis Research, 48*(3), 385–393. https://doi.org/10.1007/BF00029471
42. Nishimori, R., Mizoguchi, T., Tamiaki, H., Kashimura, S., & Saga, Y. (2011). Biosynthesis of unnatural bacteriochlorophyll *c* derivatives esterified with α, ω-diols in the green sulfur photosynthetic bacterium *Chlorobaculum tepidum*. *Biochemistry, 50*(36), 7756–7764. https://doi.org/10.1021/bi200994h
43. Saga, Y., Hayashi, K., Mizoguchi, T., & Tamiaki, H. (2014). Biosynthesis of bacteriochlorophyll *c* derivatives possessing chlorine and bromine atoms at the terminus of esterifying chains in the green sulfur photosynthetic bacterium *Chlorobaculum tepidum*. *Journal of Bioscience and Bioengineering, 118*(1), 82–87. https://doi.org/10.1016/j.jbiosc.2013.12.023
44. Saga, Y., Hayashi, K., Hirota, K., & Tamiaki, H. (2015). Modification of the esterifying farnesyl chain in light-harvesting bacteriochlorophylls in green sulfur photosynthetic bacteria by supplementation of 9-decyn-1-ol, 9-decen-1-ol, and decan-1-ol. *Journal of Photochemistry and Photobiology A: Chemistry, 313*, 44–51. https://doi.org/10.1016/j.jphotochem.2015.05.002
45. Wang, Y., Freund, D. M., Magdaong, N. M., Urban, V. S., Frank, H. A., Hegeman, A. D., & Tang, J.K.-H. (2014). Impact of esterified bacteriochlorophylls on the biogenesis of chlorosomes in *Chloroflexus aurantiacus*. *Photosynthesis Research, 122*(1), 69–86. https://doi.org/10.1007/s11120-014-0017-5
46. Zupcanova, A., Arellano, J. B., Bina, D., Kopecky, J., Psencik, J., & Vacha, F. (2008). The length of esterifying alcohol affects the aggregation properties of chlorosomal bacteriochlorophylls. *Photochemistry and Photobiology, 84*(5), 1187–1194. https://doi.org/10.1111/j.1751-1097.2008.00312.x
47. Pšenčík, J., Torkkeli, M., Zupčanová, A., Vácha, F., Serimaa, R. E., & Tuma, R. (2010). The lamellar spacing in self-assembling bacteriochlorophyll aggregates is proportional to the length of the esterifying alcohol. *Photosynthesis Research, 104*(2–3), 211–219. https://doi.org/10.1007/s11120-010-9541-0
48. Nishimori, R., Tamiaki, H., Kashiyama, S., & Saga, Y. (2015). *In vitro* self-assembly of bacteriochlorophyll *c* derivatives monoesterified with α, ω-diols isolated from the green sulfur photosynthetic bacterium *Chlorobaculum tepidum*. *Supramolecular Chemistry, 27*(1–2), 28–36. https://doi.org/10.1080/10610278.2014.904515
49. Tamiaki, H., Michitsuji, T., & Shibata, R. (2008). Synthesis of zinc bacteriochlorophyll-*d* analogues with various 17-substituents and their chlorosomal self-aggregates in non-polar organic solvents. *Photochemical & Photobiological Sciences, 7*(10), 1225–1230. https://doi.org/10.1039/B802359J
50. Huber, V., Sengupta, S., & Würthner, F. (2008). Structure–property relationships for self-assembled zinc chlorin light-harvesting dye aggregates. *Chemistry – A European Journal, 14*(26), 7791–7807. https://doi.org/10.1002/chem.200800764
51. Saga, Y., Nakai, Y., & Tamiaki, H. (2009). Temperature-dependent spectral changes of self-aggregates of zinc chlorophylls esterified by different linear alcohols at the 17-propionate. *Supramolecular Chemistry, 21*(8), 738–746. https://doi.org/10.1080/10610270902853035
52. Sengupta, S., & Würthner, F. (2012). Covalently stabilized self-assembled chlorophyll nanorods by olefin metathesis. *Chemical Communications, 48*(46), 5730–5732. https://doi.org/10.1039/c2cc32314a
53. Shoji, S., Hashishin, T., & Tamiaki, H. (2012). Construction of chlorosomal rod self-aggregates in the solid state on any substrates from synthetic chlorophyll derivatives possessing an oligomethylene chain at the 17-propionate residue. *Chemistry – A European*

Journal, 18(42), 13331–13341. https://doi.org/10.1002/chem.201201935
54. Miyatake, T., Takamori, Y., & Yamaguchi, K. (2015). Synthesis of zinc chlorin–spiropyran dyads and their self-aggregation properties. *Journal of Photochemistry and Photobiology A: Chemistry, 313*, 36–43. https://doi.org/10.1016/j.jphotochem.2015.06.017
55. Takahashi, N., Tamiaki, H., & Saga, Y. (2013). Synthesis and self-assembly of amphiphilic zinc chlorophyll derivatives possessing a crown ether at the 17-propionate residue. *Tetrahedron, 69*(18), 3638–3645. https://doi.org/10.1016/j.tet.2013.03.015
56. Tamiaki, H., Nishiyama, T., & Shibata, R. (2007). Self-aggregation of zinc chlorophylls possessing perfluoroalkyl chains in fluorous solvents: Selective extraction of the self-aggregates with fluorous phase and accelerated formation of the ordered supramolecules in this phase. *Bioorganic & Medicinal Chemistry Letters, 17*(7), 1920–1923. https://doi.org/10.1016/j.bmcl.2007.01.044
57. Shibata, R., Mizoguchi, T., Inazu, T., & Tamiaki, H. (2007). Self-aggregation of synthetic zinc chlorophyll derivatives possessing multi-perfluoroalkyl chains in perfluorinated solvents. *Photochemical & Photobiological Sciences, 6*(7), 749–757. https://doi.org/10.1039/B702866K
58. Shibata, R., Koike, K., Hori, H., & Tamiaki, H. (2008). Self-aggregation of synthetic zinc chlorophyll derivatives possessing fluoroalkyl chains in liquid carbon dioxide as models of green photosynthetic bacterial antennae. *Chemistry Letters, 37*(5), 532–533. https://doi.org/10.1246/cl.2008.532
59. Wasielewski, M. R., & Svec, W. A. (1980). Synthesis of covalently linked dimeric derivatives of chlorophyll *a*, pyrochlorophyll *a*, chlorophyll *b*, and bacteriochlorophyll *a*. *The Journal of Organic Chemistry, 45*(10), 1969–1974. https://doi.org/10.1021/jo01298a043
60. Miyatake, T., Tamiaki, H., Holzwarth, A. R., & Schaffner, K. (1999). Artificial light-harvesting antennae: Singlet excitation energy transfer from zinc chlorin aggregate to bacteriochlorin in homogeneous hexane solution. *Photochemistry and Photobiology, 69*(4), 448–456. https://doi.org/10.1111/j.1751-1097.1999.tb03311.x
61. Smith, K. M., Goff, D. A., & Simpson, D. J. (1985). *Meso* substitution of chlorophyll derivatives: Direct route for transformation of bacteriopheophorbides *d* into bacteriopheophorbides *c*. *Journal of the American Chemical Society, 107*(17), 4946–4954. https://doi.org/10.1021/ja00303a021
62. Ma, L., & Dolphin, D. (1996). Nucleophilic reaction of 1,8-diazabicyclo[5.4.0]undec-7-ene and 1,5-diazabicyclo[4.3.0]non-5-ene with methyl pheophorbide a. Unexpected products. *Tetrahedron, 52*(3), 849–860. https://doi.org/10.1016/0040-4020(95)00944-2
63. Pandey, R. K., Sumlin, A. B., Constantine, S., Aoudia, M., Potter, W. R., Bellnier, D. A., Henderson, B. W., Rodgers, M. A., Smith, K. M., & Dougherty, T. J. (1996). Alkyl ether analogs of chlorophyll-*a* derivatives: Part 1. Synthesis, photophysical properties and photodynamic efficacy. *Photochemistry and Photobiology, 64*(1), 194–204. https://doi.org/10.1111/j.1751-1097.1996.tb02442.x
64. Tamiaki, H., Takeuchi, S., Tsudzuki, S., Miyatake, T., & Tanikaga, R. (1998). Self-aggregation of synthetic zinc chlorins with a chiral 1-hydroxyethyl group as a model for in vivo epimeric bacteriochlorophyll-*c* and *d* aggregates. *Tetrahedron, 54*(24), 6699–6718. https://doi.org/10.1016/S0040-4020(98)00338-X
65. Kataoka, Y., Shibata, Y., & Tamiaki, H. (2012). Supramolecular energy transfer from photoexcited chlorosomal zinc porphyrin self-aggregates to a chlorin or bacteriochlorin monomer as models of main light-harvesting antenna systems in green photosynthetic bacteria. *Bioorganic & Medicinal Chemistry Letters, 22*(16), 5218–5221. https://doi.org/10.1016/j.bmcl.2012.06.066
66. Zhang, L., Wang, T., Jiang, J., & Liu, M. (2023). Chiral porphyrin assemblies. *Aggregate, 4*(1), e198. https://doi.org/10.1002/agt2.198